HELSINGIN YLIOPISTO
HELSINGFORS UNIVERSITET
UNIVERSITY OF HELSINKI

Characterization of a novel photosynthetic auxiliary protein PPD8 in stress reactions of *Arabidopsis thaliana*

University of Helsinki
Faculty of Biological and Environmental Sciences
Master's Programme in Plant Biology
Master's thesis

May 2020

Jasmin Kemppinen
Supervisor: Alexey Shapiguzov

HELSINGIN YLIOPISTO

Tiedekunta - Fakultet - Faculty	Laitos - Institution - Department	
Bio- ja ympäristötieteellinen	n/a	
Tekijä - Författare - Author		
Jasmin Kemppinen		
Työn nimi - Arbetets titel		
Fotosynteettisen apuproteiini PPD8:n rooli lituruohon stressireaktioissa		
Oppiaine - Läroämne - Subject		
Kasvibiologia		
Työn laji/ Ohjaaja - Arbetets art/Handledare - Level/Instructor	Aika - Datum - Month and year	Sivumäärä - Sidoantal - Number of pages
Pro gradu -tutkielma / Alexey Shapiguzov	05/2020	72 s + x liitteet.

Tiivistelmä - Referat - Abstract

Fotosynteesissä syntyvät happiradikaalit (radical oxygen species, ROS) toimivat usein ensimmäisinä signaaleina stressaavissa olosuhteissa, kuten esimerkiksi voimakkaassa valossa. Tumassa sijaitseva säätelyproteiini RADICAL-INDUCED CELL DEATH1 (RCD1) on herkkä kloroplastissa syntyville happiradikaaleille, jonka seurauksena tuma aloittaa muun muassa vaihtoehtoisten oksidaasien (alternative oxidase, AOX) ja muiden hapetus-pelkistystasapainoa ylläpitävien komponenttien luennan kasvisolussa. Kloroplasti voi akklimoitua myös hyvin nopeasti muuttuviin valo-olosuhteisiin jo ennen geeniekspression muuttamista, esimerkiksi tasapainottamalla fotosysteemien kykyä vastaanottaa valoenergiaa ja lisäämällä ylimääräisen eksitaatioenergian poistamista lämpöväreilynä (t.s. ei-valokemiallinen vaimentaminen; non-photochemical quenching, NPQ). Näissä nopeissa tapahtumissa toimii lukuisia pieniä apuproteiineja, joista suuri osa on havaittu vasta geenitasolla. Pro gradu -tutkielman tavoitteena on kuvailla aiemmin hypoteettisen apuproteiini PPD8:n toimintaa lituruohossa (Arabidopsis thaliana), PPD8:n yhteistyötä RCD1:n sekä tioredoksiinireduktaasin (NTRC) kanssa hapetus-pelkistys-tasapainon ylläpitämiseksi sekä varmistaa PPD8:n ilmentyminen kasvissa.

Poistamalla lituruoholta geenit PPD8, RCD1 ja NTRC sekä risteyttämällä linjat keskenään loimme kaksois- sekä kolmoismutantit rcd1 ppd8 ja ppd8 rcd1 ntrc. Kaskoismutanttien sekä yksittäisten poistogeenisten linjojen (ppd8, rcd1 ja ntrc) fenotyyppejä vertailtiin tutkimalla eri proteiinien ilmentymistä western blot –menetelmällä sekä mittaamalla kloroplastien fluoresenssia kahdella eri tavalla. Mutanttien solukoita altistettiin voimakkaasti hapettavalle parakvatille (methyl viologen, MV) ja siten lisääntyneille happiradikaaleille sekä hapellisissa että hapettomissa olosuhteissa. Mittaamalla kloroplastien fluoresenssia kahdella eri tekniikalla (PAM ja uuden sukupolven kuvallinen OJIP) saatiin tietoa millisekuntien aikaskaalalla elektroninsiirtoketjun tapahtumista. Lisäksi loimme kloonaamalla T-DNA-insertiolinjan, jossa PPD8 –proteiiniin lisättiin merkkiaineeksi hemagglutiniinia (HA) koodaava geeni proteiinin havaitsemiseksi kasvissa.

Poistogeeninen rcd1 on tunnetusti hyvin kestävä happiradikaaleja vastaan, mutta risteyttämällä linja ppd8:n kanssa saatiin aikaan happiradikaaleille herkkä mutantti. Sekä rcd1 ppd8 että ppd8 osoittivat hyvin korkeita klorofyllifluoresenssin ja ei-valokemiallisen vaimentamisen tasoja. PPD8-geenin poistaminen vaikutti kasvien fotosynteettisten proteiinien ekspressioon sekä stoikiometriaan heikentäen merkitsevästi fotosynteettistä kapasiteettia. Kun RCD1, NTRC ja PPD8 poistettiin kasvista, tuloksena oli äärimmäisen heikko linja, jonka NPQ- ja fluoresenssitasot olivat merkitsevästi korkeammat kuin muilla tutkimuksen kasveilla. Lisäksi useat tuloksistamme viittasivat mahdollisesti vioittuneeseen ATP-syntaasin toimintaan ppd8 linjoissa. Esitämme, että PPD8 on olennainen fotosynteettisen koneiston optimaaliselle toiminnalle. HA-insertiolinjalla voitiin myös muuntaa täysin poistogeeninen ppd8 linja fenotyypillisesti villityypiksi, mikä varmisti proteiinin ilmentymisen kasvissa.

Avainsanat - Nyckelord

Kasvifysiologia, *Arabidopsis thaliana*, fotosynteesi, klorofyllifluoresenssi, oksidatiivinen stressi, kloroplasti, RCD1, NTRC

Säilytyspaikka - Förvaringsställe - Where deposited

HELDA - Helsingin yliopiston digitaalinen arkisto

Muita tietoja - Övriga uppgifter - Additional information

HELSINGIN YLIOPISTO

Tiedekunta - Fakultet - Faculty	Laitos - Institution - Department	
Faculty of Biological and Environmental Sciences	n/a	
Tekijä - Författare - Author		
Jasmin Kemppinen		
Title		
Characterization of a novel photosynthetic auxiliary protein PPD8 in stress reactions of *Arabidopsis thaliana*		
Oppiaine - Läroämne - Subject		
Plant biology		
Työn laji/ Ohjaaja - Arbetets art/Handledare - Level/Instructor	Aika - Datum - Month and year	Sivumäärä - Sidoantal - Number of pages
Master's Thesis / Alexey Shapiguzov	05/2020	72 p + x appendices

Tiivistelmä - Referat – Abstract

Reactive oxygen species (ROS) are one of the prominent groups of signal compounds that are produced in stress conditions such as excess light. Nuclear protein RADICAL-INDUCED CELL DEAT (RCD1) is sensitive to ROS and controls the expression of organelle components, e.g. mitochondrial alternative oxidases (AOX), thus balancing the redox-status of a plant cell. Plants have fast responses to fluctuating light conditions that happen even before gene expression: i.e. readjusting the capability to receive light energy between the two photosystems by state transitions and increasing the capacity to remove excess energy by non-photochemical quenching (NPQ). Various small auxiliary proteins function in these fast acclimation events. However, many of them are identified on gene level only. The goal of this master's thesis is to describe the role of a hypothetical protein, PPD8 in *Arabidopsis thaliana*. We evaluate how PPD8 is associated with RCD1 and a chloroplast thiol-regulator enzyme NTRC.

We created double (*rcd1 ppd8*) and triple mutant plant lines (*rcd1 ppd8 ntrc*) by crossing single knockout lines *ppd8*, *rcd1* and *ntrc.* Photosynthetic performance, NPQ and sensitivity to ROS were observed in each line by using two different chlorophyll fluorescence measurement methods: pulse-amplitude-modulation (PAM) and novel OJIP imaging fluorometry. The leaves were exposed to methyl viologen (MV), which accelerates the chloroplastic ROS production in light, and also to hypoxic conditions in order to study how the effect of MV is altered in low concentrations of oxygen. Additionally, we examined the amount of photosynthetic proteins and stoichiometry of photosystems in *ppd8*, *rcd1* and *rcd1 ppd8* by immunological methods. Finally, *PPD8* gene with attached hemagglutinin encoding tags was generated by cloning and reintroduced back to the *ppd8* knockout lines.

Plants lacking *RCD1* are very tolerant against MV and ROS, but when *rcd1* was crossed with *ppd8* the resistance was suppressed. Both *rcd1 ppd8* and *ppd8* exhibited elevated chlorophyll fluorescence and NPQ values. The removal of *PPD8* gene had an impact on the abundance and the stoichiometry of photosynthetic proteins reducing the plants' performance. When *RCD1*, *PPD8* and *NTRC* were simultaneously absent the plants had major defects: their NPQ and fluorescence values were drastically increased. Furthermore, several results hinted towards possible issues in the function of ATP synthase in *ppd8* background plants. It is also known that NTRC regulates ATP synthase: taken together, the results suggest that PPD8 is necessary for a fully operative ATP synthase and photosynthetic machinery. By reintroducing *PPD8* to knockout line *ppd8*, the phenotype could be reverted back to wild type -like, thus confirming the significance of the *PPD8* gene product in plant.

Keywords

Plant physiology, *Arabidopsis thaliana*, photosynthesis, chlorophyll fluorescence, oxidative stress, chloroplast, RCD1, NTRC

Säilytyspaikka - Förvaringsställe - Where deposited

HELDA - Digital Repository of the University of Helsinki

Muita tietoja - Övriga uppgifter - Additional information

Contents

Abbreviations **1**

1 Introduction **2**

2 Background **5**

2.1 Light-dependent reactions of chloroplasts 5

2.1.1 Linear electron flow *7*

2.1.2 Photosystems and auxiliary proteins *8*

2.2 Regulation of energy balance and redox poise in light-dependent reactions 11

2.2.1 Chlorophyll fluorescence *12*

2.2.2 Non-photochemical quenching *14*

2.2.3 Cyclic electron flow *15*

2.2.4 State transitions *16*

2.2.5 Thioredoxin systems *17*

2.3. Reactive oxygen species (ROS) in chloroplasts and organellar redox signaling 18

2.3.1 Retrograde signaling from chloroplast *19*

2.3.2 RCD1 and organellar cross-talk *20*

3 Preceding work and research questions **22**

4 Materials and methods **24**

4.1 Plant material and growing conditions 24

4.2 DNA extraction from plant material 24

4.3 Cloning 25

4.3.1 Isolation and elution of PPD8 genomic sequence *26*

4.3.2 Generation of entry and expression clones *27*

4.3.3 Transformation into Escherichia coli *27*

4.3.4 Plasmid DNA extraction from E. coli *28*

4.3.5 Agrobacterium tumefasciens transformation and infiltration *28*

4.3.6 Surface sterilization of seeds *29*

4.3.7 Growing A. thaliana in vitro and selection for hygromycin resistant plants *29*

4.4 Chlorophyll fluorescence imaging 30

4.4.1 PAM *30*

4.4.2 OJIP *30*

4.5 Isolation, separation and detection of proteins and protein complexes 31

4.5.1 Immunological methods *31*

4.5.2 Separation of thylakoid protein complexes *32*

4.6 Statistical analysis and data presentation 32

5 Results **33**

5.1 Generation of *rcd1 ppd8* 33

5.2 Complementation of *ppd8* and *rcd1 ppd8* 34

5.3 Defects in NPQ 36

5.4 Photosynthetic phenotypes of *ppd8* 38

5.5 Phenotypes of *rcd1 ppd8 ntrc* 40

5.6 PPD8 is not related to mitochondrial functions of *rcd1* and is partially redundant with NTRC 43

6 Discussion **46**

7 Conclusions **52**

8 Acknowledgements **53**

9 References **54**

10 Appendices **69**

Abbreviations

CEF	Cyclic electron flow
Fo, Fm	Minimal and maximal chlorophyll fluorescence
Fs	Chlorophyll fluorescence under light
Fv	Variable fluorescence (Fm – Fo)
g_{H+}	Conductivity of a biological membrane for protons
LEF	Linear electron flow
LHCII / LHCII-P	Light harvesting complex II / Phosphorylated light harvesting complex II
NPQ	Non-photochemical quenching
OJIP	Fo-Fj-Fi-Fp kinetics of chlorophyll fluorescence rise
PAM	Pulse amplitude modulation fluorometry
PCR	Polymerase chain reaction
ϕRE1o	Quantum yield of the electron flux to PSI electron acceptors
Pmf	Proton motive force
PsaB	PSI core subunit
PsbA	D1, PSII core subunit
PSI	Photosystem I
PSII	Photosystem II
RCD1	Radical induced cell death 1

1 Introduction

Photosynthetic organisms are the foundation of biodiversity on Earth. Without their capability to convert light energy into chemical energy, the diversity of species would be very limited in comparison to the abundance of life today.

Photosynthesis is a photochemical reaction that has been evolving for billions of years in cyanobacteria, algae and green plants. Briefly, photosynthetic light reactions use light energy to draw out electrons from water molecules for cellular metabolism. This stage of photosynthesis is occurring in specialized organelles called chloroplasts, which diverged from cyanobacteria over 1.2 billion years ago in an endosymbiotic event (Mereschkowsky 1905, Douglas 1998, Delwiche 1999, Matsuzaki et al. 2004, McFadden and van Dooren 2004). Chloroplasts' inner membrane structures called thylakoids harbor protein complexes, which carry out the electron transfer reactions. Their overall structure and function is well established, but the regulatory events and components that contribute to the plants' ability to acclimate to varying light conditions are yet to be fully unravelled. The more genomic data we acquire the less we seem to know – approximately 15 % of plants' nuclear gene products may be of cyanobacterial origin and targeted to chloroplasts (Deusch et al. 2008).

The energy of light drives charge separation inside photosystems, which triggers a series of redox reactions such as splitting of water into oxygen, protons and electrons, and electron transfer chain. To capture light, the plants use pigments. Chlorophyll, one the most important constituents of photosystems and light-harvesting antennae, absorbs mostly red and blue wavelengths. Excitation of chlorophyll molecules is under tight control, because excessive light energy can be damaging for the cell. Impairment can happen if e.g. oxygen atom functions as an acceptor for the electrons, thus creating reactive oxygen species (ROS) that are unstable and can potentially damage other molecules. Plants have three means for getting rid of this excessive energy: by I) dissipation it as heat energy, i.e. non-photochemical quenching (NPQ), II) Förster resonance energy transfer to another molecule, and III) fluorescence. In other words, the energy that cannot be harnessed into chemical energy or dissipated

as heat can be observed via fluorescence. Chlorophyll fluorescence measurement is a powerful tool for inspecting the events that happen in the light reactions at different time scales.

Plants must respond to fluctuating light conditions rapidly. The fastest responses, e.g. NPQ, state transitions and photosystem repair occur at the site of photosynthesis without changes in gene expression. As a longer-term adaptation strategy, plant cell initiates molecular signaling pathways that lead to changes in gene expression. Recent evidence suggests that not only signaling from plastids to nucleus and gene expression is necessary for efficient photosynthesis but also reciprocal communication between organelles of different types, e.g. chloroplasts and mitochondria, seems to be instrumental in maintaining energy metabolism (Blanco et al. 2014, Shapiguzov et al. 2020). So-called retrograde signals from plastids to nucleus can carry information via different mechanisms, e.g. through molecular modifications caused by the altered redox status of chloroplast enzymes. These enzymes may affect metabolism of ROS. Despite their harmful potential, ROS are now considered as crucial molecular signals, however the exact mechanisms of ROS signalling in different cellular events are not yet completely understood. It is proposed that ROS signaling is frequently converted to thiol redox exchange signal, changes in calcium fluxes, modified signal molecules, alterations in metabolite pools, etc. How plants can differentiate distinctive ROS sources and initiate corresponding responses is one of the major enigmas in plant physiology.

One central protein that binds together chloroplastic, mitochondrial and nucleo-cytosolic redox signals is RADICAL-INDUCED CELL DEATH 1 (RCD1) (Overmyer et al. 2000, Shapiguzov et al. 2019). *Arabidopsis thaliana* exhibits peculiar phenotypes when *RCD1* gene is removed, such as tolerance to methyl viologen (MV), a herbicide that accelerates ROS production in the chloroplast (Fujibe et al. 2004). From this premise, Kangasjärvi's research group conducted a genetic screen in order to find genes that could revert this MV tolerance of *rcd1*. Several candidate lines were found. A number of them demonstrated high chlorophyll fluorescence phenotypes. In one of such lines the causative gene was suggested to be *PPD8* (At5g27390) (Järvi et al. 2013). Consequently, one

of the research questions of this thesis is if *PPD8* is implicated in MV tolerance. Here, we show that the absence of *PPD8* is indeed affecting MV tolerance of plants. We also performed intensive biochemical and spectroscopic studies of photosynthesis in *ppd8* mutants. From the obtained results we gathered evidence for a presumptive role of PPD8.

The background chapter explores the fundamental theories regarding photosynthesis, chlorophyll fluorescence, fast acclimation in response to light, redox maintenance systems, ROS and organellar signaling. The perspective on this theoretical section is on how it relates to the research techniques that are used in the thesis. Another focus is on the accessory proteins of chloroplast in higher plants because previous studies and bioinformatic predictions suggest that *PPD8* encodes an undetected, putative auxiliary protein with an unknown function (Sato 2010, Järvi et al. 2013). Additionally, the role of RCD1 and regulatory chloroplastic thiol enzymes are underlined. The third chapter summarizes the basis of this study, the preceding work, and the research questions accompanied by our hypotheses. Chapter four covers the methods and materials: instruments, reagents, plant material and growth conditions as well as the protocols. The results are presented and interpreted in chapter five, followed by discussion and concluding remarks.

2 Background

The underlying mechanisms that regulate photosynthesis have been under extensive inspection since the plants were observed to affect their environment in the mid 17th century. Jan van Helmont first demonstrated that plants consumed water from the soil in 1796. Later, Joseph Priestley conducted his famous experiments with oxygen including the observations that plants can produce compounds that kept a candle burning in a sealed dome when exposed to light (Rabinowitch, 1945). During the last century these discoveries were confirmed: indeed, green plants produce oxygen from water in a reaction called photosynthesis. Oxygenic photosynthesis evolved at least 2.4 billion years ago in an ancestor of cyanobacteria, which descendants reside in plant cells today as organelles called chloroplasts (Mereschkowsky, 1905; Douglas & Raven, 2003; Cardona et al. 2015). Photosynthesis has an invaluable role as the basis for terrestrial biodiversity, and undoubtedly, is one of the main reasons why plants make up to 80% of all biomass on Earth (Hohmann-Marriot & Blankenship, 2011; Bar-On et al., 2018).

2.1 Light-dependent reactions of chloroplasts

The photosynthetic events occur in chloroplasts' internal membranes called thylakoids (figure 1). Chloroplasts have two functionally and morphologically differing inner membrane systems: stroma and grana thylakoids (figure 1A). Grana thylakoids form stacked and cylindrical structures that are bound together by stroma lamellae. These stroma thylakoids are exposed to stromal liquid of the chloroplasts from both sides and are helically bound around cylindrical grana thylakoids, which in turn consist of 5-20 layers of thylakoid membrane (Mustárdy et al. 2008). All thylakoid membranes in a chloroplast encapsulate a single, continuous lumenal space (Shimoni et al. 2005).

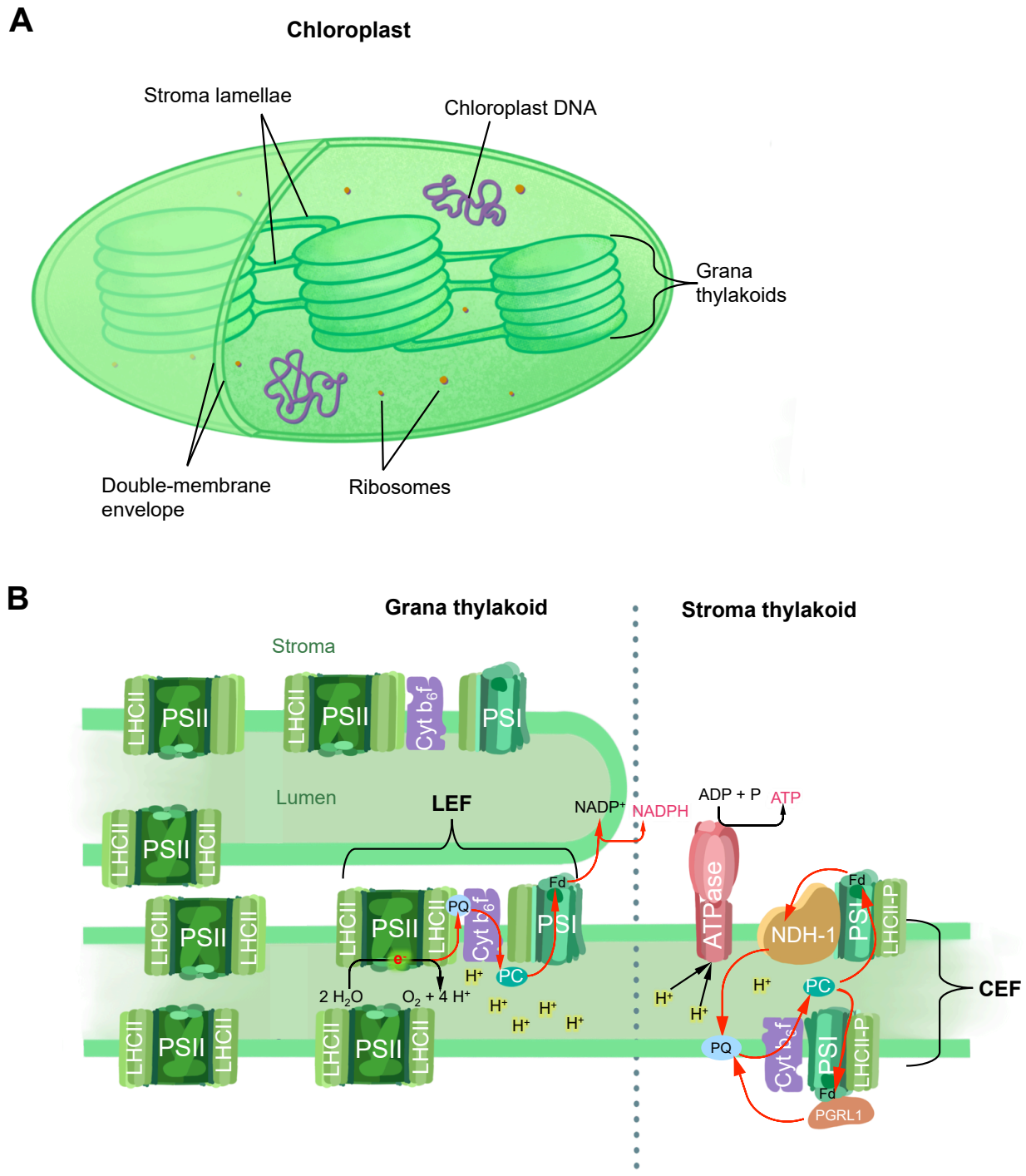

Figure 1. Chloroplast and its structures. (**A**) Components of a typical chloroplast. The double membrane envelope surrounds stroma fluid and internal membrane systems called thylakoids. Two types of thylakoids are shown: stroma lamellae and stacked grana thylakoids. (**B**) Cross section of grana and stroma thylakoids reveals the lateral heterogeneity in the distribution of photosystems, ATP-synthase and cytochrome b_6f complex. Red arrows represent the major routes of electron flow: linear electron flow (LEF) and cyclic electron flow (CEF). In LEF, the electrons reduce the final acceptor $NADP^+$, forming NADPH. Both routes transfer protons (H^+) into the lumen. Proton gradient is utilized by ATP-synthase in phosphorylation of ADP into ATP. Scheme is adapted from *Oxygenic Photosynthesis — Light Reactions within the Frame of Thylakoid Architecture and Evolution* (Järvi et al. 2017).

The thylakoid membranes contain protein complexes that carry out the electron transfer and proton translocation reactions: photosystem II (PSII), photosystem I (PSI), cytochrome b_6f complex (cyt b_6f), ATP synthase, NADH dehydrogenase (NDH) complex as well as the light harvesting complex II (LHCII) and other accessory proteins (figure 1B). These photosynthetic complexes are not evenly dispersed throughout the thylakoid membranes but differ in their abundance and distribution across stroma lamellae and grana stacks (Andersson and Anderson, 1980; Albertsson, 2001; Dekker and Boekema, 2005; Nevo et al., 2012). This uneven distribution of photosynthetic proteins is called lateral heterogeneity: grana thylakoids contain mostly PSII whereas stroma thylakoids are rich in PSI and ATP synthase.

2.1.1 Linear electron flow

Originally, light energy excites electrons in pigment molecules in the light-harvesting antenna complexes around photosystems. Excited electrons (also called “excitons”) travel though resonance energy transfer to the reaction center, which is the two dimeric chlorophyll *a* pigments in the PSII core called P680 by the peak wavelength of its absorption spectrum (Konermann and Holzwarth 1996). The charge separation occurs in P680, i.e., the excited electron leaves P680, which turns into P680+. As the strongest known biological oxidant, P680+ provides energy for the oxidation of water molecule into gaseous oxygen, protons and electrons (Rappaport et al. 2002). Two water molecules are oxidized in five different stages called the Kok cycle (Kok et al. 1970). The extracted electrons are accepted sequentially by special tyrosine Z, which transports them to P680+. The electrons that left P680 after charge separation reduce the plastoquinone (PQ): the mobile lipid-soluble isoprenoid quinol molecules that transport electrons in their reduced form (plastoquinol, PQH_2) along thylakoid membranes to the next acceptor, cytochrome b_6f complex (Cramer et al. 2006, Müh et al. 2012). Plastoquinone pool acts as one of the major redox hubs in thylakoids, which affects the photosynthetic rate. These and other regulatory events are described in 2.2.

The reduced plastoquinol transfers electrons in two phases of the so-called Q-cycle that involves the cytochrome b_6f complex, a plastoquinol-plastocyanin oxidoreductase (Cramer et al. 2006). At its lumenal site, PQH_2 donates two electrons: one for PQ, hence forming semi-plastoquinone and another for plastocyanin through cyt b_6f complex. Plastocyanin is a mobile electron carrier protein soluble in thylakoid lumen and acting as an electron donor for the PSI reaction center (P700) (Haehnel et al. 1994). The terminal electron acceptor in PSI is ferredoxin (Fd), which together with ferredoxin NADP+ reductase (FNR) reduce NADP+ into NADPH, a vital molecule yielding reducing power that is used in carbohydrate synthesis of the Calvin-Benson cycle and many other cellular reactions (Tagawa and Arnon 1962, Edwards and Walker 1983).

The journey of an electron from water to different acceptors serves several functions: firstly, it creates reducing power and secondly, it translocates protons from stroma to lumen. The generated chemical potential (ΔpH) together with the membrane electrical potential (ΔΨ) create proton motive force (*pmf*), which is utilized by ATP synthase in the phosphorylation of ADP into ATP (Hangarter and Good 1982, Armbruster et al. 2017). Additionally, ΔpH is essential for the activation of a photoprotective mechanism called non-photochemical quenching (NPQ), which is described in detail in 2.2.2.

2.1.2 Photosystems and auxiliary proteins

PSII is comprised of 25-35 transmembrane and peripheral proteins that have essential functions in the PSII assembly and repair cycles. The core of PSII consists of the central subunits D1 and D2, internal antenna proteins CP43 and CP47, in addition to large amount of low-molecular mass subunits (Boekema et al. 1995, Miyao and Murata 1984). The oxgen-evolving complex (OEC) drives the oxidation of water and resides in the lumenal side of PSII: it is a Mn_4CaO_5 cluster surrounded by multiple extrinsic subunits (Ifuku and Noguchi 2016, Roose et al. 2016). From these, at least PsbO, PsbP and PsbQ are fundamental for efficient photosynthesis in higher plants (Suorsa and Aro 2007, Bricker et al. 2012). They optimize the oxygen evolution and shield Mn_4CaO_5 cluster from exogenous reductants.

The abundance of oxygen and the capability of creating redox potential of up to 1.3 V bring constant oxidative pressure on PSII (Ishikita et al. 2005). Indeed, PSII core complex D1 is prone to biochemical damage and has a rapid turnover rate (Aro et al. 1993, Mulo et al. 2012). Therefore, correct expression and assembly of photosystems are crucial in the prevention of photo-oxidative damage and –inhibition. Photosynthetic organisms have evolved exceptional repair mechanisms for the PSII reaction center, i.e. monomerization and partial disassembly of the core complex, replacement of the impaired D1 with a fresh subunit and reassembly (Aro et al 2005). Interestingly, all the different steps of the repair process exist in the chloroplast simultaneously (Danielsson et al. 2006). This repair cycle of PSII is assisted by various auxiliary proteins, such as members of the heat shock protein family of 70 kDa (HSP70) (Schroda et al. 1999, Yokthongwattana et al. 2001), albino (ALB) protein family members (Sundberg et al. 1997, Kuhn et al. 2003), soluble stromal protein Psb29 (Keren et al. 2005), lumenal protein Psb27 (Nowaczyk et al. 2006) and many others. Additionaly, the extrinsic subunits are suggested to be of great importance in the assembly of OEC during the fast reassembly (Ettinger and Theg 1991, Hashimoto et al. 1997). One of the model for the OEC assembly, called the “regulatory cap” model proposes that PsbO binds to the lumenal side of PSII and provides a docking site for PsbP, which further associates PsbQ (Miyao and Murata 1989). Alternative models for OEC assembly are suggested but the role of PsbO, PsbP and PsbQ remain emphasized. Additional low-molecular-mass (LMM) proteins are also present in the stable association of OEC in higher plants, i.e. PsbL, PsbJ and PsbR, whose roles were addressed by reverse genetics approaches (Suorsa et al. 2004, 2006).

Auxiliary subunits of photosystems frequently have several homologs in higher plants. In *Arabidopsis*, nuclear-encoded PsbP and its eight homologs accumulate in the thylakoid lumen (Roose et al. 2007). PsbP family proteins are divided into categories based on their amino-acid sequence similarities with PsbP: two PsbP-like proteins (PPL) and six PsbP-domain proteins (PPD) (Ishihara et al. 2007). Additional members of the PsbP family are known as PPD7

and PPD8; however, they have not been detected in proteomic studies (Sato 2010, Järvi et al. 2013).

In comparison to the extensive knowledge of the function, subunits and biogenesis of PSII, the assembly of PSI is not as well understood. PSI also has a complex organization, as it is one of the largest bioenergetic complexes known (Ifuku et al. 2011). In higher plants, PSI consists 15 subunits (PsaA-PsaL and PsaN-PsaP) in addition to the at least four light harvesting complexes (LHCA1-4) that form the PSI antenna (Amunts et al. 2010). Together PsaA and PsaB form the reaction center of PSI, and several auxiliary proteins called assembly factors are involved in the formation of mature PSI core. Similarly to PSII, many auxiliary proteins involved in PSI assembly are identified from mutant screens (Schöttler et al. 2011). LHCI proteins are known to be involved in the supercomplex formation of PSI-NDH (Peng et al. 2009). These supercomplexes play a major role in cyclic electron flow, which is described in 2.2.3.

Excitation energy is transferred to the reaction centers through internal and peripheral antenna complexes (Cao et al. 2018). Peripheral antenna complex of PSII consists of three major subunits and three minor subunits, which together form light harvesting complex II (LHCII) (Jackowski et al. 2001). LHCII is an important factor in balancing the excitation states of PSII and PSI: these so-called state transition events are described in 2.2.4. In addition to LHCII, some smaller auxiliary proteins also function as energy-balancing actors in changing light environment. One important PSII subunit of higher plants called PsbS operates as a lumenal pH sensor that activates non-photochemical quenching (NPQ) for emitting excess excitation energy as heat (Li et al. 2000). NPQ and other energy balance maintenance systems are summarized in the following subchapter.

2.2 Regulation of energy balance and redox poise in light-dependent reactions

Light-induced excitation of molecules must be under a degree of regulation in order to prevent excess energy and formation of harmful excitation. All excited pigment molecules can be hazardous for the cell if their energy levels arise uncontrollably. For example, chlorophyll has several reactive excitation states: i. a short-lived singlet state where electrons have antiparallel spins ii. longer-lived triplet state with electrons that have parallel spins (figure 2A). Triplet chlorophyll has potential to form singlet oxygen, a reactive species of oxygen that may interact with organic molecules causing damage to e.g thylakoid membrane lipids (Krieger-Liszkay 2005). Accessory pigments such as carotenoids can act as reactive oxygen quenchers, i.e they act as antioxidants (Lee and Min 1990). If these protective antioxidant systems fail, photodamage can occur. Ultimately photodamage may lead to photoinhibition, in which the excessive light energy reduces the photosynthetic capacity.

Plants have three means for getting rid of this potentially harmful excessive excitation energy of the pigment molecules: by i. dissipation as heat energy ii. Förster resonance energy transfer from one molecule to another, and iii. fluorescence (figure 2A). The heat dissipation is called non-photochemical quenching (NPQ). In Arabidopsis NPQ depends on the auxiliary protein PsbS, which modifies interactions between PSII and antenna proteins in light-dependent way. These mechanisms in addition to chlorophyll fluorescence and other redox energy-balancing strategies are examined in this chapter.

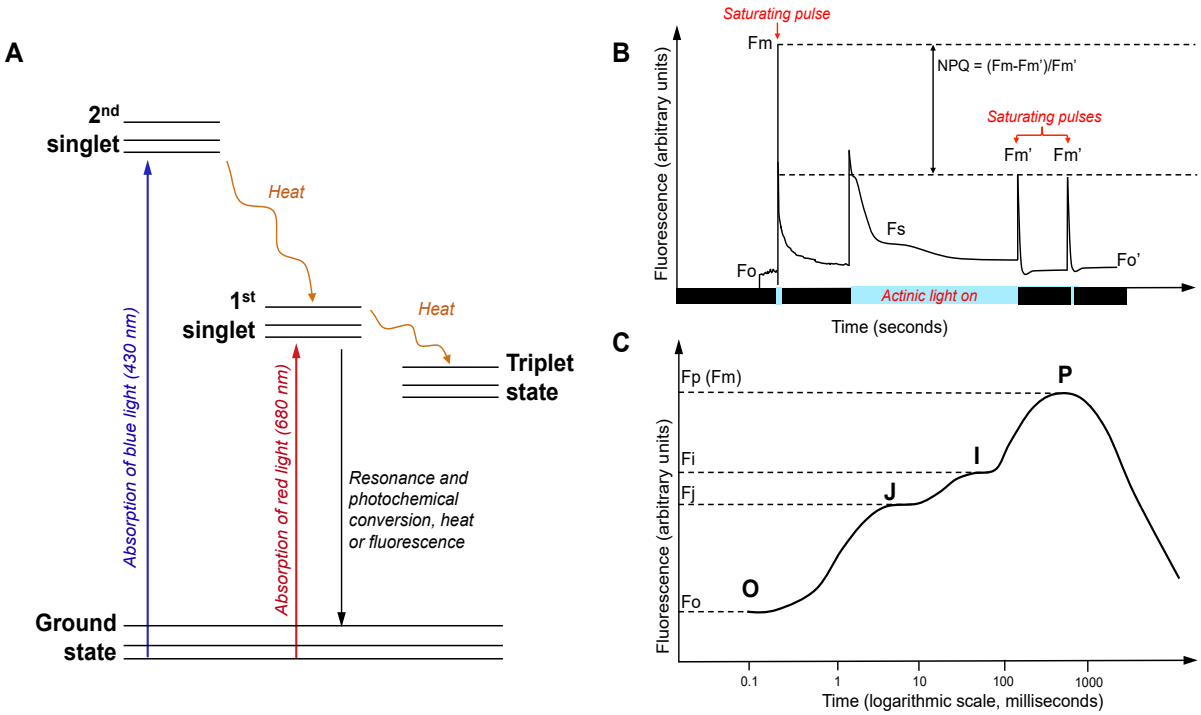

Figure 2. Basics of chlorophyll excitation states, energy transfer and fluorescence. (**A**) Diagram showing the energy states of chlorophyll molecule. Conversion from the second excited state to the first excited state emits heat, whereas the excitation energy from the first singlet state can be converted to photochemical energy. Excess excitation energy can be emitted as heat, fluorescence or it can increase the possibility of triplet state chlorophyll formation. Triplet chlorophyll molecule may produce reactive and harmful singlet oxygen. (**B**) Representation of a pulse-amplitude-modulation (PAM) experiment with key parameters. Black bars indicate darkness and blue bars display light. (**C**) Typical OJIP transient obtained from dark-adapted samples. Different redox steps in the LEF can be interpreted from the phases shown in the OJIP-transient. For details, see the text (2.2.1).

2.2.1 Chlorophyll fluorescence

Chlorophyll *a* has two absorption peaks: one at red (680 nm) and one at blue (430 nm) wavelenghts (figure 2A) (Brody and Brody, 1961). If the absorbed energy cannot be transferred to another molecule, it can be dissipated as heat and/or via fluorescence. Chlorophyll fluorescence originates mainly from the PSII: when the dark-adapted leaf is illuminated, a following rapid but slowly declining rise in fluorescence can be observed. This phenomenon called the Kautsky effect was first discovered in 1960 by Kautsky et al.

Chlorophyll fluorescence can be a powerful tool for inspecting the events that occur in the light reactions at different time scales ranging from microseconds to hours or days. In order to use measurements of chlorophyll fluores-

cence for e.g photosynthesis efficiency, the difference between photochemical quenching and non-photochemical quenching must be distinguished. This is achieved by terminating photochemistry, which allows fluorescence measurements in the presence of non-photochemical quenching alone (figure 2B). To block photochemical quenching, a high intensity, short flash of light is applied to the leaf. This transiently closes all PSII reaction centres, which prevents energy of PSII being passed to downstream electron carriers. Non-photochemical quenching will not be affected if the flash is short. During the flash, the fluorescence of dark-adapted plants reaches the level reached in the absence of any photochemical quenching, known as maximum fluorescence Fm (Baker 2008).

The efficiency of PSII can be estimated by comparing (Fm) to the yield of variable fluorescence (Fv) in the light (Fv/Fm) and the yield of fluorescence in the absence of light (Fo) (Schreiber et al. 1995). Alterations in NPQ change values of maximum fluorescence since the development of NPQ is light-dependent (Kanazawa and Kramer 2002). Thus, to measure the yield of chlorophyll fluorescence in absence of NPQ the plants should be adapted to darkness.

Different chlorophyll fluorescence parameters such as the efficiency of PSII and NPQ are usually measured with pulse-amplitude-modulation (PAM) fluorometry. Figure 2B presents a typical PAM experiment with saturation pulses and the calculation of NPQ. However, even the quicker events can be examined, such as the fluorescence rise of a dark-adapted leaf from Fo to Fm which usually takes ~0.3 s (Strasser and Strasser 1995). When plotted on a logarithmic time scale, this induction curve appears with its characteristic phases: fluorescence steps Fo, Fj, Fi and Fp (figure 2C). This so-called OJIP transient is usually interpreted in the following manner: the first, “open state” (Fo) is the minimum fluorescence when all the PSII reaction centers are open and the electron transport chain is ready to accept an excited electron, thus only minimal amount of fluorescence can be observed. The second state, Fj, is the first platform of the fluorescence curve. The fluorescence rise from Fo-Fj is due to the readily closing primary PQ acceptor sites of the PSII reaction center (i.e. Q_A sites) as the plastoquinone pool gets reduced (Tsimilli-Michael and Strasser 2013, Strasser et al. 2005). The Fj-Fi phase of the curve correlates with the reduction

of the secondary acceptor PQ (Q_B), PQ and Cyt b_6f and PC. Finally, the Fi-Fp part corresponds to the reduction of final electron acceptors of PSI, such as Fd and NADP+. The Fp is the peak plateau observed from the OJIP kinetics – all possible acceptors are fully reduced.

Previously, OJIP kinetics have been measured by using either nonimaging methods (Stirbet 2011) or by using so-called “pump-and-probe” (P&P) principle, where the transients were acquired discontinuously with series of flashes (Jedmowski and Brüggermann 2015). However, due to the newly developed ultrafast camera technologies, continuous measurement and imaging of the OJIP transient is now possible (Küpper et al. 2019). These new technologies allow the analysis of heterogeneity of the fluorescence kinetics in different plant tissues and the elimination of measurement artifacts when compared to the P&P method.

After the fast OJIP transient a slow decrease in the kinetics can be observed. This relaxation in fluorescence is referred to as the slow phase, which occurs in a time frame of secods to tens of minutes (Papageorgiou 1968, Schansker et al. 2006) and is related to the activation of non-photochemical quenching, state transitions and other adjustments.

2.2.2 Non-photochemical quenching

When all reaction centers are closed, fluorescence can still be quenched due to non-photochemical quenching. NPQ is amongst the fastest responses of the photosynthetic machinery to excess light (Govindjee et al. 2014). The mechanisms of NPQ rely on various factors in the photosynthetic processes, most importantly the function and composition of light harvesting antenna complexes, the status of reaction centers, the activity of electron transport, and proton gradient (Walker 1987, Ruban 2013).

The NPQ can be calculated as (Fm/Fm′) – 1 (Bilger and Björkman 1990, Baker 2008) and it consists of several components: qE, which is the major and fastest component of NPQ that is set off by increasing ΔpH (Ruban 2013), and qZ, which is related to the formation of zeaxanthin in a process called xantho-

phyll cycle (Demmig-Adams et al. 1987, Nilkens et al. 2010) and qI that is associated with irreversible inhibition of PSII.

NPQ takes place on the light-harvesting antenna. Generally, ΔpH buildup in the lumenal space affects LHCII, monomeric antenna complexes and violaxanthin de-epoxidase and importantly the PsbS protein (Ruban et al. 2012). PsbS acts as a proton-sensitive “switch” that turns the LHCII antenna into NPQ state, possibly by conformational changes (Horton et al. 2005). When activated, LHCII complexes rearrange/aggregate as well as change their pigment composition for more efficient thermal dissipation of excess light energy. Importantly, carotenoids, especially the xanthophyll zeaxanthin, are essential in the development of NPQ (Niyogi et al. 1998, Nilkens et al. 2010).

It would seem straightforward that LEF was the major contributor to the activation of NPQ since it pumps protons into the lumen. However, plants have another mechanism for proton translocation across the thylakoid membrane: cyclic electron flow, which appears to be crucially responsible for ΔpH and is even proposed to make up the largest portion of NPQ (Munekage et al. 2004). Additionally, Sato et al. (2014) revealed that the ΔpH generated by the cyclic electron flow contributes 60 % - 80 % to NPQ formation.

2.2.3 Cyclic electron flow

Cyclic electron flow (CEF) around PSI (figure 1B) acts as an alternative mechanism to allocate protons into the lumen in addition to LEF. There are several proposed routes for CEF and all of them function as secondary electron acceptors from PSI: CEF pathways can cycle electrons from NADPH or reduced ferredoxin back to PQ pool (Fork and Herbert 1992, Heber and Walker 1993). CEF is essential for operative photosynthesis as it prevents the over-reduction of Fd pool and potential production of ROS that can damage FeS centers of PSI (Endo et al., 1999; Munekage et al. 2004; Tiwari et al., 2016).

Two main mechanisms for CEF are proposed: I) NADH dehydrogenase (NDH) dependent route and II) a pathway mediated by two proteins called PROTON GRADIENT REGULATION 5 (PGR5) and PGR5 LIKE PHOTOSYNTHETIC PHENOTYPE (PGRL1) (Matsubayashi et al., 1987; Munekage et al.,

2004; DalCorso et al., 2008; Peltier et al., 2016). The activity of these alternative routes is dependent on redox state of stroma (Breyton et al., 2006). For example, NDH complex is regulated by thiol group modifications by chloroplast thioredoxins, such as NADPH-thioredoxin reductase (NTRC) (Courteille et al., 2013; Nikkanen et al., 2018). Thioredoxin systems are described in more detail in section 2.2.5.

NDH was originally discovered when 11 plastid genes were confirmed to be homologs of genes encoding subunits for mitochondrial NDH dehydrogenase complex (complex I) (Matsubayashi et al., 1987). Consisting of at least 29 subunits, NDH is known as one of the largest protein complexes (~ 700 kD) in the photosynthetic electron transport chain (Peng and Shikinai 2011, Ifuku et al. 2011). NDH regulates CEF arond PSI by transfering electrons from ferredoxin to PQ pool (Yamamoto et al. 2011, Yamamoto and Shikinai 2013). NDH forms even larger supercomplex with PSI (Järvi et al., 2011). CEF mediated by NDH is suggested to protect PSI from oxidative damage in rice, and it seems to be a crucial factor for normal growth under low light conditions (Yamori et al. 2015, 2016). Another protein complex that can initiate CEF is PGR5 with a second protein PGRL1 (Munekage et al., 2002, DalCorso et al., 2008). When oxidized, PGR5 is associated with PGRL1. As PGR5 is reduced by electrons from ferredoxin it donates them to PGRL1 and dissociates from it. Reduced PGRL1 transfers the electrons to cytochrome b_6f complex, thus to PQ and eventually to PSI.

2.2.4 State transitions

The most abundant membrane protein complex on Earth, the light harvesting complex II (LHCII) forms trimers that hold at least half of all the chlorophyll pigments in chloroplasts (Kühlbrandt et al. 1994, Liu et al. 2004). LHCII is under tight regulation: it can be phosphorylated by Stt7/STN7, a serine/threonine-protein kinase that is activated upon the reduction of the plastoquinone pool (Vener et al. 1997, Zito et al. 1999). Phosphorylated LHCII detaches from PSII and is then bound to PSI, maintaining the energy balance between the photosystems (Depège et al. 2003, Lemeille et al. 2009). This state transition event is reversible by the PPH1/TAP38 phosphatase that dephosphorylates PSI-bound

LHCII thus allowing its transition back to PSII (Shapiguzov et al. 2010). The transition event is regulated by redox balance between the photosystems and is one of the fastest adaptations to differing light conditions (Wollman 2001, Kargul and Barber 2008, Tikkanen et al. 2010, Lemeille and Rochaix 2010). Additionally, the phosphorylation status of LHCII can act as a useful indicator of the redox balance between the two photosystems since the phosphorylation of the LHCII complex can be assessed via immunological methods. Abnormal LHCII phosphorylation may mark defects in the PSII/PSI stoichiometry or NADPH/ATP ratio etc.

2.2.5 Thioredoxin systems

Plants have various mechanisms for monitoring the redox status of the photosynthetic machinery and thus the light conditions. A group of regulatory proteins called thioredoxins (TRXs) control several cellular events such as cyclic electron flow and Calvin-Benson cycle (Buchanan et al. 2002). TRXs are protein oxidoreductases that regulate the structure and function of proteins by reducing the disulphide bond between the side chains of two cysteine residues. Oxidized thioredoxins are reactivated by thioredoxin reductases (TR) (Schürmann and Jacquot 2000). Of the the two plastid thioredoxin systems, ferredoxin-dependent system relays reducing equivalents from PSI via ferredoxin and ferredoxin-thioredoxin reductase (FTR) to chloroplast thioredoxins and then to diverse thioredoxin target proteins (Droux et al. 1987, Schürmann and Buchanan 2008). The second system relies on NADPH-dependent thioredoxin reductase of type C (NTRC) (Serrato et al. 2004). This protein includes an NADPH-thioredoxin reductase and a thioredoxin domain in a single polypeptide. NTRC can be activated either in light conditions by photosynthetic NADPH or in the darkness by NADPH from oxidative pentose phosphate pathway (OPPP) (Neuhaus and Emes 2000). NTRC is important regulator of proteins involved in photosynthesis as well as a protective factor against oxidative damage (Pérez-Ruiz et al. 2006). NTRC has been shown to reduce the antioxidant 2-Cys peroxiredoxin system (Puerto-Galán et al. 2015), the enzymes involved in chlorophyll biosynthesis (Richter et al. 2013) and starch biosynthesis (Michalska et al. 2009). Further-

more, NTRC activates NDH-dependent CEF (Nikkanen et al. 2018) as well as regulates ATP synthase (Carrillo et al. 2016).

2.3. Reactive oxygen species (ROS) in chloroplasts and organellar redox signaling

Despite chloroplasts' protective mechanisms the charge separation can and ultimately does result in formation of undesirable metabolic products. The most reactive and potentially damaging compounds are of oxygenic origin, called the reactive oxygen species (ROS). These compounds were previously considered to be mere by-products of light reactions and mitochondrial electron transport events. Although ROS can cause damage to organic compounds they are now widely studied as signaling molecules (Kangasjärvi et al. 2012, Shapiguzov et al. 2012). Indeed, generation of ROS such as singlet oxygen ($^1O_2$), superoxide (O_2^-), hydroxyl radical ($^{\bullet}OH$), and most importantly hydrogen peroxide (H_2O_2) are frequently the first signs of various abiotic and biotic stresses. For example, pathogen attack rapidly induces ROS formation at the site of infection where it can act as a signal for initiating the programmed cell death (PCD) (Kroemer et al. 1995, Morel and Dangl 1997, Overmyer et al. 2003). ROS signalling is commonly accompanied by calcium ion signalling and can propagate from cell to cell initiating a systemic signal (Kobayashi et al. 2007, Miller et al. 2009).

In plants, the majority of ROS are formed in the chloroplastic light reactions, mainly at two sites: at PSII and at PSI. Singlet oxygen can be created by P680 chlorophyll triplet state that has been produced via radical pair recombination or by accessory chlorophylls via intersystem crossing (ISC) (Macpherson et al. 1993). Singlet oxygen is highly reactive and can damage the PSII reaction center protein D1, thus causing photoinhibition (Trebst et al. 2002, 2004; Krieger-Liszkay 2005). PSII can also produce superoxide, which too can cause photoinhibition (Zulfugarov et al. 2014). However, several studies have proposed that oxidative photoinhibition may be primarily caused by ROS suppressing *de novo* biosynthesis of D1 through inactivation of the thioredoxin-regulated elon-

gation factor G, rather than by the oxidative degradation of the D1 (Kojima et al. 2007, Nishiyama et al. 2011).

PSI can also be subjected to photoinhibition and oxidative damage. In the PSI, the most commonly produced ROS is the superoxide (Sonoike 1996). In optimal conditions, the main primary electron acceptor from P700 is the ferredoxin-FNR-complex that further reduces the NADP+ into NADPH. However, superoxide can also occasionally be formed under high light conditions if the oxygen molecule acts as the electron acceptor (Asada et al.1973). Superoxide is quickly dismutated by superoxide dismutase (SOD) to form H_2O_2. The reduction of oxygen to form H_2O_2 in chloroplasts was first discovered by Mehler in 1951. This reaction, called Mehler reaction is the first step of a chloroplast Water-water cycle (WWC), in which WWC converts H_2O_2 into water by using the reducing power of ascorbate (Asada 2000). Thus, WWC provides an additional protective mechanism in excessive light conditions in coordination with ascorbate-glutathione cycle.

2.3.1 Retrograde signaling from chloroplast

Cells of photosynthesizing eukaryotes including plants carry a unique combination of energy-producing organelles: mitochondria and chloroplasts. Moreover, plant cells retain three types of DNA: nuclear (nDNA), plastid (cpDNA) and mitochondrial (mtDNA). Most of organellar DNA has been incorporated into the nDNA after the endosymbiotic events. Moreover, chloroplasts and mitochondria can modulate the expression of nuclear genes through different signaling mechanisms called retrograde signals. The origin and chemical nature of these signals can vary a lot. Some studied retrograde signals are RNA molecules (Bradbeer et al. 1979), transcription factor proteins such as Whirly 1 (Isemer et a. 2012), metabolites like porphyrin precursors (Strand et al. 2003), plant hormones e.g. ABA (Baier and Dietz 2005), carotenoid oxidation products like β-cyclocitral (Ramel et al. 2012) and ROS, most importantly singlet oxygen and hydrogen peroxide (Apel and Hirt 2004).

As said, ROS itself can act as a retrograde signal from chloroplast; however, due to the short life span of these molecules only H_2O_2 mainly diffuses

outside the organelle. Rather, plant organelles relay information about their redox status by accumulating metabolites that are caused by ROS production, like β-cyclocitral. One chloroplastic retrograde signal that has been studied in the context of oxidative stress is called 3′-phosphoadenosine 5′-phosphate (PAP): this molecule can translocate from chloroplast to the nucleus and initiate the expression of plastid redox associated nuclear genes (PRANGs) (Estavillo et al. 2011). PAP accumulates under stress conditions, especially under high light. In normal conditions, PAP is enzymatically degraded by SAL1 phosphatase, but during chloroplast ROS production SAL1 is inactivated and the accumulation of PAP initiates changes in gene expression trough retrograde signalling (Chan et al. 2016).

2.3.2 RCD1 and organellar cross-talk

Another important regulatory protein especially in the context of oxidative stress is called RADICAL-INDUCED CELL DEATH1 (RCD1). RCD1 is a nuclear protein that contains a WWE, a poly ADP-ribose polymerase-like (PARP-like), and a C-terminal RCD1-SRO1-TAF4 (RST) domain (Overmyer et al. 2000, Ahlfors et al. 2004, Jaspers et al. 2009, Jaspers et al., 2010a). RCD1 is sensitive to ROS: chloroplastic ROS likely leads to inactivation of RCD1 in the nucleus (Shapiguzov et al. 2019) (figure 3). There, RCD1 acts as a negative regulator of transcription factors ANAC013 and ANAC017. These two transcription factors mediate a ROS-related signal from mitochondrial electron transport chain (De Clercq et al. 2013, Ng et al. 2013, Van Aken et al. 2016b). When electron leakage occurs on the mitochondrial electron transport chain, ANAC proteins migrate into the nucleus where they activate the expression of mitochondrial dysfunction stimulon genes (*MDS*) (De Clercq et al. 2013, Van Aken et al. 2016a), which include i.e. mitochondrial alternative oxidases (*AOX*). Expression of *MDS* genes is always upregulated in *rcd1*.

Plants lacking RCD1 have a very distinctive phenotype. For example, *rcd1* is very tolerant to methyl viologen, a compound that accelerates ROS production by PSI i.e. enhancing the Mehler reaction (Fujibe et al., 2004). The reasons for this are not yet quite clear but they could be related to decreased availability of

molecular oxygen by the electron-acceptor side of PSI, possibly due to altered mitochondrial respiration (Shapiguzov et al. 2020). Another notable phenotype of the *rcd1* is increased thiol redox state of its chloroplast enzymes, including NTRC. Chloroplastic ROS are known to act as electron sink for chloroplast thiol redox enzymes. For this reason it could be that this phenotype of *rcd1* is related to its MV tolerance.

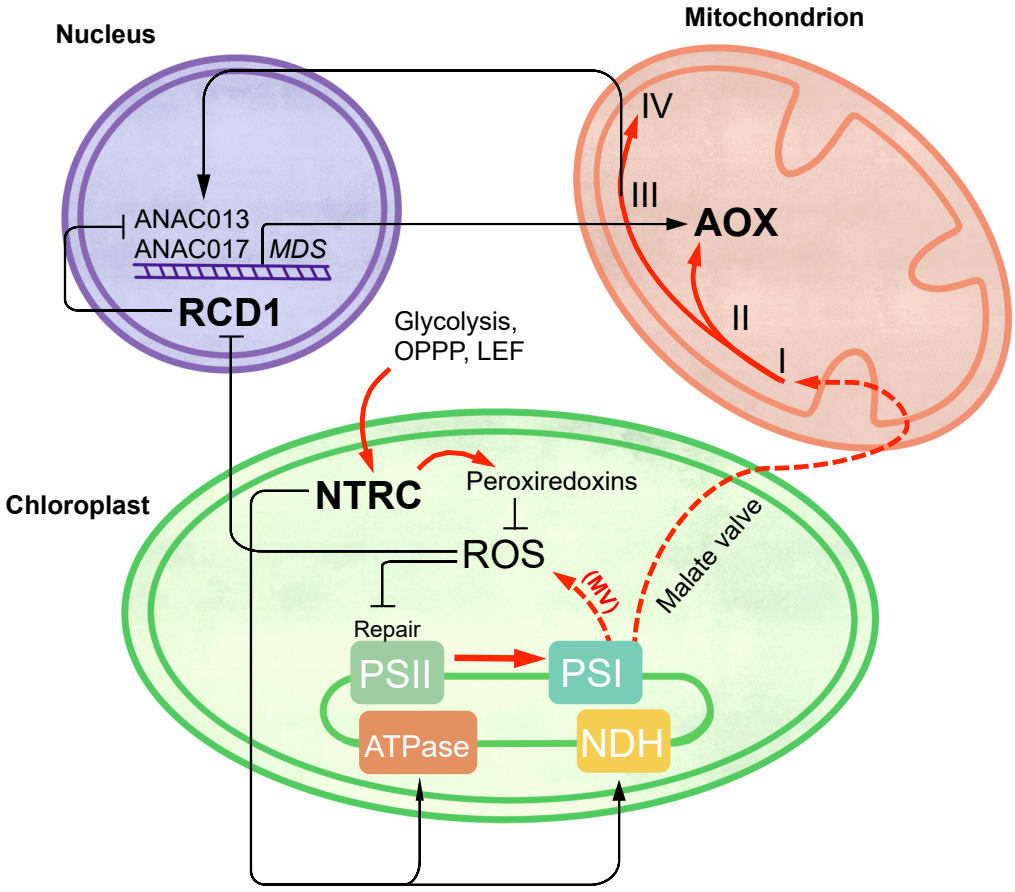

Figure 3. RADICAL-INDUCED CELL DEATH1 (RCD1) converges the redox signaling networks between nucleus, mitochondria and chloroplasts (Shapiguzov et al. 2019). Electron transfer pathways are presented with red arrows, whereas black arrows and flat-ended lines indicate activation and inhibition. Alterations in mitochondrial respiration initiate the expression of nuclear mitochondrial dysfunction stimulon (*MDS*) genes, which gene products include alternative oxidases (AOX). Expression of *MDS* is suppressed by RCD1, which in turn is sensitive to ROS produced in the chloroplast. ROS production via Mehler's reaction can be induced by MV. ROS are scavenged by e.g. peroxiredoxins, which are recharged and reduced by NADPH-thioredoxin reductase (NTRC). NTRC regulates various events in chloroplasts, such as the activity of ATP-synthase and NADH dehydrogenase-like complex (NDH). The redox balance of mitochondria and chloroplasts is interconnected through malate valves, RCD1, the activity of AOX and, possibly, through O_2 exchange between the organelles (Shapiguzov et al. 2020).

3 Preceding work and research questions

RCD1 is the plant-specific nuclear protein that controls, among other processes, energy metabolism in chloroplasts and mitochondria (Shapiguzov et al. 2019, Shapiguzov et al. 2020). Kangasjärvi research group has studied RCD1 extensively. The basis of this study was the tolerance of *rcd1* knockout plants' against methyl viologen (MV) and chloroplastic ROS production. In order to dissect this phenotype, an ethyl methanesulfonate (EMS)-induced mutagenesis screen was carried out in *Arabidopsis thaliana rcd1*-mutant background (figure 4A). Candidate plants with restored sensitivity to high light and MV were isolated (figure 4A and B), after which possible causative genes were found by genome resequencing. From this screen, several candidate lines with reduced tolerance to MV were isolated, among them line #28 (figure 4C). Genomic sequence analysis was carried out in line #28, revealing several possible causative mutations. One of these mutations was the defect in the coding region of gene At5g27390, a.k.a *PPD8*.

A

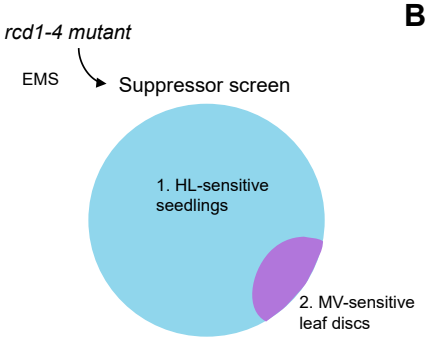

B

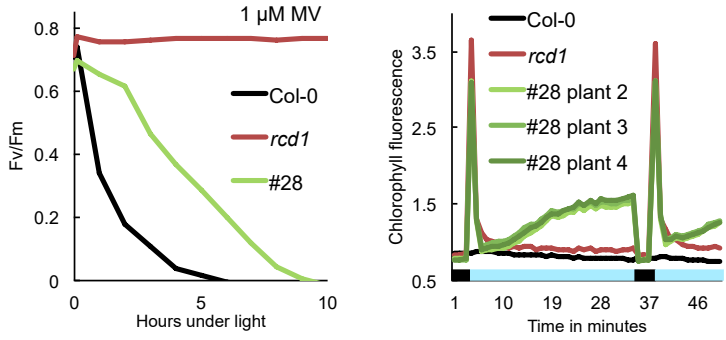

C

Candidate	Gene	Annotation
#28.1	AT5G27390	Mog1/PsbP/DUF1795-like photosynthesis; chloroplast
#28.2	AT5G26330	Cupredoxin superfamily, electron carrier activity, copper ion binding
#28.3	AT5G26580	AGAMOUS-LIKE-34; type I member of MADs box domain transcription factor family; nucleus.

Figure 4. The outline of the *rcd1* suppressor screen. (**A**) Knockout *rcd1-4* plants were mutated with EMS and then screened for sensitivity to high light. From high light sensitive seedlings MV-sensitive plants were selected for further analysis. (**B**) Left panel: decreasing PSII efficiency Fv/Fm showed that screen candidate line #28 exhibited sensitivity for 1 μM MV during exposure to light (146 µmol photons m^{-2} s^{-1}). Right panel demonstrates chlorophyll fluorescence (normalized to minimum fluorescence Fo) of three individual plants from line #28 that were highly fluorescent under actinic light (blue bar). (**C**) Different candidate lines, their mutated gene loci and annotations from TAIR (The Arabidopsis Information Resource). Independent T-DNA knockout-lines with

disrupted candidate genes were ordered and their MV tolerance and habitus were investigated. Knocking out At5G27390, later called *PPD8*, lowered MV tolerance the most when compared to other knockout lines, thus this gene was chosen for further examination in this study.

Plants of the candidate line #28 possessed not only decreased MV tolerance, but also peculiar chlorophyll fluorescence phenotypes (figure 4B, right panel). Some of these changes were likely caused by the defects of the background *rcd1* mutant, some by the second site mutation, putatively *ppd8*. The *rcd1*-specific changes in photosynthesis largely depend on the chloroplast master regulatory thiol enzyme NTRC (Shapiguzov et al. 2020). Thus, in my project I evaluated photosynthetic performance of single and higher order *ppd8*, *rcd1* and *ntrc* knockout mutants.

From this basis, the following research questions were asked in my study:

1. Does inactivation of *PPD8* cause similar suppressor phenotypes as those observed in the screen line #28?
2. Does re-introduction of *PPD8* gene revert the phenotypes of *ppd8* or *rcd1 ppd8* mutants?
3. In which ways are *ppd8* plants compromised, why do they have high chlorophyll fluorescence and what are the presumptive roles of PPD8?
4. What is the role played by PPD8 in the context of *rcd1* and what is the functional link between PPD8 and NTRC?

4 Materials and methods

4.1 Plant material and growing conditions

Arabidopsis thaliana wild type of ecotype Col-0 and knockout lines *rcd1-4* (GK-229D11), *ntrc* (SALK 096776) and *ppd8* (SAIL 249 E03) were used in this study. The *ppd8* line was obtained from the Nottingham Arabidopsis Stock Centre (NASC; http://arabidopsis.info/BasicForm). Seeds were sown on soil (1:1 peat:vermiculite) and vernalized in 4 °C for two days. Plants were then transferred to 12 h photoperiod growth rooms with constant relative humidity of ~60%, 23 °C day / 19 °C temperatures and light intensity of 220–250 μmol photons per m^{-2} s^{-1}. The plants were grown for seven to ten days before transplanting to fresh soil. Each experiment was conducted on 3-5 week old plants.

We generated double mutants *rcd1 ppd8, rcd1 ntrc* and *rcd1 ppd8 ntrc* by crossing *rcd1* with *ppd8* and *ntrc.* The triple mutant *rcd1 ppd8 ntrc* was a cross between *rcd1 ppd8* and *rcd1 ntrc.* The crossing was carried out on as described by Rivero et al. (2014).

Each F2 plant's genotype was confirmed by PCR with corresponding primers (listed in appendix 1). For an individual reaction, we used 1 μl of genomic DNA, 0.5 μl (10 μM) of each of the two primers, 0.3 μl of FIREPol® DNA Polymerase by Solis Biodyne, 2 μl of FIREPol buffer, 0.5 μl DNA nucleotides (10 mM) and 15.2 μl of distilled water. The PCR program was run with following cycles and temperatures: denaturing at 95 °C, annealing at 59 °C and synthesis at 72 °C. DNA extraction from plant material is described in 3.2. Finally, 8 μl of 6 x DNA Loading dye by Thermo Fisher Scientific was added to PCR reaction mix samples which were then separated on 1% agarose gel with x 0.5 TAE buffer and ethidium bromide. Gene Ruler 1kb Plus DNA Ladder (Thermo Scientific) was used for the reference fragment size.

4.2 DNA extraction from plant material

From each plant line, a small leaf (~ 4 x 4 mm) was collected into safelock eppendorf with forceps that were wiped with water and ethanol between each

sample. Leaf samples were frozen (-20 °C) and ground with 500 µl of DNA extraction buffer (100 mM Tris pH 7.8, 50 µM EDTA, 50 mM NaCl) and glass beads (100 µl) in a safelock eppendorf by shaking (16 000 rpm) the samples three times for 30 seconds with five-second intervals in a triturator (Silamat S5 or Ivoclar Vivadent AG). Samples were then centrifuged for 10 minutes at 13 000 rpm, after which 400 µl of supernatant was pipetted into fresh tubes with 500 µl of 100% isopropanol. Tubes were gently mixed by turning them upside down. DNA was let to precipitate for 10 minutes at room temperature followed by 10 minutes of 13 000 rpm centrifugation. Supernatant was discarded and 400 µl of 70% ethanol was added. Sample was again centrifuged (10 minutes in 13 000 rpm) and supernatant was removed. DNA was dried by leaving the eppendorf lid open on 37°C heating block for 10 minutes or until no liquid was left. After drying, 30 µl of distilled water was added to dissolve DNA. The purity and concentration of DNA were measured by using a Nanodrop spectrophotometer (Thermo Fisher Scientific).

4.3 Cloning

Genomic sequence of *PPD8* with a native promotor (5997 bp upstream from the start codon) was amplified from Col-0 genomic DNA using the primers GW-PPD8-promoter-F (GGGG ACA AGT TTG TAC AAA AAA GCA GGC T CAG-CAAAACACATCTCAATA) and GW-PPD8-CDS-R (GGGG AC CAC TTT GTA CAA GAA AGC TGG GT TTAGAATAGTGAAAGAAATGG). The obtained fragment was introduced to the pGWB13 destination vector using step-wise Gateway reactions (Invitrogen) as described below. The final plasmid construct (figure 5) encoded PPD8 with three hemagglutinin epitopes in the C-terminus and had two antibiotic resistance genes: hygromycin resistance for selection in plants and kanamycin resistance for bacterial selection. This vector was introduced to knockout lines *ppd8* and *rcd1 ppd8* by Agrobacteria-mediated floral dipping (Zhang et al. 2006).

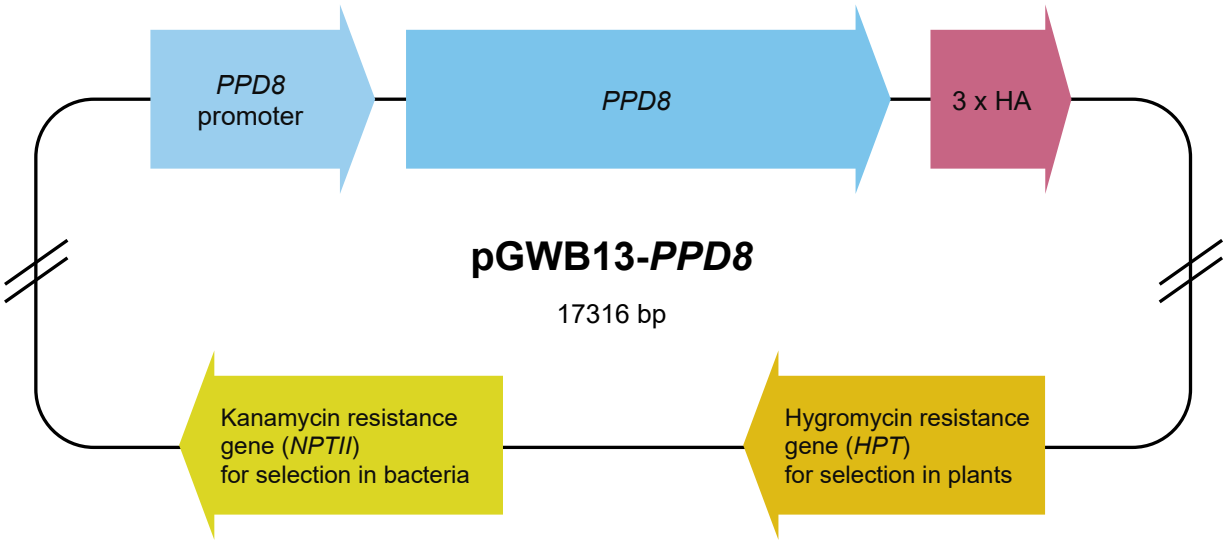

Figure 5. 17 316 base pairs in size, the vector carried three hemagglutinin (HA) coding sequences in C-terminus of *PPD8*. Chloroplastic proteins that are encoded in the nucleus contain N-terminal signal peptides called transit peptides, which are cleaved out by stromal processing peptidase after imported to the chloroplast. PPD8 is encoded in the nucleus and presumably targeted to chloroplast by transit peptides that are cleavable – thus, we added HA-tags to the C-terminus of *PPD8.*

4.3.1 Isolation and elution of *PPD8* genomic sequence

We isolated DNA from Col-0 plants in order to acquire genomic sequence of *PPD8*. DNA was extracted from WT plant as described in 3.2. We used ApE plasmid editor program by M. Davis to design primers flanking the CDS of *PPD8* including the native promotor. Primers were ordered from Sigma-Aldrich. We used Phusion® High-Fidelity DNA polymerase by Thermo Fisher Scientific for PCR. For amplification, we added 4.5 µl forward and 4.5 µl reverse primers (10 µM each) to 6 µl of Phusion enzyme, 40 µl Phusion buffer, 5 µl of DNA nucleotides, 0.5 µl of WT Col-0 genomic DNA and 147 µl distilled water. The PCR program had four 98 °C – 51 °C – 72 °C temperature cycles followed by 35 temperature cycles of 98°C – 60 °C – 72 °C.

PCR product was isolated from 1 % agarose gel by cutting the corresponding band with a sterile scalpel. The gel fragment was put into 0.5 ml eppendorf, which had a small needle-punctured hole in the bottom and contained ~100 µl glass wool. The 0.5 ml eppendorf was placed into a larger 1.5 ml eppendorf. The tubes were centrifuged at 6000 rpm for 10 minutes, resulting in DNA eluate in the bottom of the larger tube. Distilled water was added to the DNA until the volume was 500 µl. Then we added 50 µl of 3 M sodium acetate

(pH = 5.6) and 550 µl of isopropanol to the solution and thoroughly mixed. After 15 minutes of waiting in the room temperature the solution was centrifuged at maximum speed for 20 minutes at 4 °C. The supernatant was carefully removed, and 500 µl 70 % ethanol was added. The solution was mixed by slowly inverting the tube, after which the eppendorf was centrifuged at maximum speed for 5 minutes at room temperature. The ethanol was removed and DNA was dried and dissolved in water as in 3.2.

4.3.2 Generation of entry and expression clones

We used One Tube Format Gateway technique (Invitrogen) to combine the BP and LR reactions, which firstly transferred the gene of interest into pDONR/Zeo entry vector, and then into pGWB13 destination vector. For BP reaction we mixed 3.5 µl of DNA, 0.5 µL of entry vector pDONR/Zeo, 1 µl of BP clonase enzyme mix (Invitrogen) and 5 µl of distilled water. The reaction was performed overnight at room temperature, after which we took 2 µl aliquot to assess the efficiency of the BP reaction by later transforming the mix into *Escherichia coli* and plating the cells onto zeocin selection LB agar plates. To the remaining mix we added reagents for the LR reaction: 1 µl of destination vector pGWB13 and 1 µl of LR Clonase II enzyme mix. After 18 hours of incubation, both solutions were treated with 0.7 µl of proteinase K for 10 minutes at 37 °C to terminate the reactions.

4.3.3 Transformation into *Escherichia coli*

Competent *E. coli* strains DH5-Alpha were incubated with entry or destination vectors for 30 minutes on ice followed by 90 second heat shock at 42 °C. For 50 µl of *E. coli,* 1 µl of DNA solution from either BP or LR reactions were used. Bacterial cells were transferred back to ice for additional 10 minutes. Then, we added 1 ml of lysogeny broth (LB) without antibiotics and shook the cultures for 1 hour in 37 °C. The tubes were centrifuged at 6000 rpm for three minutes and the supernatant was discarded. Bacterial pellets were resuspended and plated on LB-plates containing antibiotics: zeocin (25 µg / mL) for entry vector selection and kanamycin (50 µg / mL) for destination vector selection. The plates

were incubated overnight at 37 °C.

4.3.4 Plasmid DNA extraction from E. coli

Grown colonies were selected from LB-plates and inoculated into 5 mL of LB with corresponding antibiotics. The tubes were shaken o/n at 37 °C. Then, the cultures were transferred into 15-mL centrifuge tubes and centrifuged for 10 minutes at 4000 rpm. Liquid medium was discarded and plasmid DNA was isolated with the help of the GeneJET Plasmid Miniprep Kit (Thermo Scientific). In brief, the bacterial pellet was resuspended in 250 µl of ice-cold alkaline solution I by vortexing. Then 250 µl of lysis solution II was added and the tube was inverted rapidly without vortexing. 350 µl of solution III was added again and the tubes were vortexed carefully in inverted position to disperse the solution evenly through bacterial lysate. The tubes were centrifuged at 14000 rpm for 10 minutes in a microcentrifuge after which the supernatants were transferred into the spin columns. DNA on the column was washed twice with the Washing Buffer as specified by the Thermo Scientific protocol and eluted with 50 µl of water into new tubes.

We checked the resulted plasmids by restriction analysis: for entry clones pDONR/Zeo we used HindII and for expression clones pGWB13 we used HindIII restriction enzymes. 0.5 µl of DNA was incubated for one hour at 37 °C with 1 µl of Hind II/Hind III, 16.5 µl distilled water and corresponding buffers by Thermo Fisher Scientific. Additionally, we sent the plasmids to StarSEQ® sequencing.

4.3.5 *Agrobacterium tumefasciens* transformation and infiltration

We added 1 µg of destination vector DNA obtained from plasmid purification to *A. tumefasciens* strain GV3101. The cells were incubated on ice for 30 minutes after adding the DNA. The cells were transformed by freezing them in liquid nitrogen and thawing on hand temperature (~ 32 °C), after which 1 ml of LB medium was added and the cells were cultivated at 28 °C with shaking for four hours. The cells were pelleted by centrifugation and plated on LB agar plates containing four antibiotics: kanamycin (50 µg / mL), hygromycin (25 µg / mL),

gentamycin (50 µg / mL) and rifampycin (20 µg / mL). The plates were incubated at 28 °C.

After three days of cultivation, two colonies were taken from plates and transferred to 5 mL of liquid LB medium with four antibiotics, as described above. The LB culture was incubated at 28 °C with shaking for 48 hours. After this, 1 mL of the culture was used to inoculate 50 mL of the same LB medium as above and further incubated overnight at 28 °C with shaking. On the next day the agrobacteria were pelleted by centrifugation and used for infecting the flowering *ppd8* and *rcd1 ppd8* plants by floral dipping according to Zhang et al, 2006.

4.3.6 Surface sterilization of seeds

Seeds were sterilized in a solution of 70% ethanol with 0,05% Triton X-100 (Sigma-Aldrich) by shaking the eppendorfs at 1400 rpm for 10 minutes. Next, the seeds were washed three times with 100% ethanol in a laminar flow cabinet. Seeds were dried on a filter paper and put on MS plates by spreading or with sterilized toothpicks.

4.3.7 Growing *A. thaliana in vitro* and selection for hygromycin resistant plants

After drying, the seeds were sown on 1 x MS basal medium (Sigma-Aldrich) with 0.5% Phytagel (Sigma-Aldrich) and 40 *µ*g/ml hygromycin. The plates were placed in 4°C temperature for two days. After vernalization, the plates were exposed to 150 *µ*E light for 5 hours and then wrapped in foil to block light allowing only the plants with hygromycin resistance gene to grow, essentially as described by Harrison et al. 2006. Plates were in darkness for 5 days and then subjected to ambient light on a laboratory bench. Plants that were resistant to hygromycin had elongated hypocotyls: these seedlings were selected and transplanted into 1:1 peat:vermiculite soil and grown in conditions as described in 4.1. We examined the expression of HA in the adult hygromycin-positive T1 plants as described in immunological methods 4.5.1.

4.4 Chlorophyll fluorescence imaging

Fluoroscopic experiments were conducted on leaf discs or plant rosettes. Each sample was let floating on distilled water solution with 0,05% Tween 20 (Sigma-Aldrich) and a given concentration of MV. For controls, we used distilled water supplemented with 0.05% Tween without MV.

4.4.1 PAM

Chlorophyll fluorescence was measured by MAXI Imaging PAM (Walz). We studied the fluorescence kinetics with saturating pulses and actinic light without the presence of MV. Leaf discs were dark adapted for one hour before exposing them to two saturating pulses (450 nm, > 3 000 µmol m $^{-2}$ s^{-1}) at the beginning of the measurement and at 5 minutes. At seven-minute timepoint actinic light (450 nm, 20 µmol m $^{-2}$ s^{-1}) was turned on and the fluorescence measurement continued for 20 minutes.

To study the effect of MV on PSII inhibition, we used a PAM protocol consisting of repetitive 1-hour periodical blue actinic light (450 nm, 80 µmol m $^{-2}$ s^{-1}). Each period was followed by a 20-minute dark adaptation and measurements of Fo and Fm. The photochemical yield of PSII was calculated as Fv/Fm = (Fm-Fo)/Fm, and the NPQ was calculated as (Fm-Fm')/F' (Baker, 2008).

4.4.2 OJIP

We used novel FluorCam FC800F from Photon Systems Instruments for OJIP fluorescence kinetics and imaging. FluorCam FC800F contains an ultra-fast sensitive CMOS camera, TOMI 3, which can acquire images with a maximum frame rate of 20 µsec. The instrument is described in more detail by Küpper et al. 2019. For parameter adjustments and data analysis we used FluorCam software. The OJIP imaging protocol was executed as in Shapiguzov et al. (2020).

4.5 Isolation, separation and detection of proteins and protein complexes

For immunoblotting and separation of photosynthetic proteins, we used plant material that was snap-frozen in liquid nitrogen. Samples were ground with glass beads in safe-lock eppendorf tubes as described in 4.2. but the tubes were kept in liquid nitrogen between grinding repeats. We used approximately two times the volume of lysis buffer (2 % SDS, 20 mM Tris-HCL, pH 7.8, and x 100 Sigma protease inhibitor cocktail from Sigma-Aldrich in distilled water) in μl for the starting amount of ground plant material in mg (2*n* μl of lysis buffer was added to *n* mg of frozen plant tissue). Samples were incubated for 20 minutes at 37 °C, shaking, and then centrifuged for 5 minutes at maximum speed. Supernatant was transferred into a new tube, which was again centrifuged for 5 minutes at maximum speed. To calculate the chlorophyll concentrations for each sample, we added green lysate from a sample to 1 ml of 80 % ice-cold acetone and mixed the solution by vortexing. The protein extracts were centrifuged at maximum speed in room temperature for 3 minutes and stored at -79 °C. Chlorophyll content was estimated essentially according to (Porra et al. 1989).

4.5.1 Immunological methods

Protein concentration was calculated by measuring the absorbance of protein samples. We equilibrated the samples by adding a calculated amount of original lysis buffer and 4x loading buffer with mercaptoethanol.

Proteins were separated by sodium dodecyl sulfate–polyacrylamide gel electrophoresis (SDS-PAGE). 12% polyacrylamide was used and the protocol was carried out according to Laemmli (1970). Before loading protein samples into wells, samples were heated with loading buffer for 15 minutes in 56 °C. After 3 minute centrifugation at maximum speed, 15 μl of each sample was loaded on the gel, which was run at > 20 mA current per one gel (and about 150 V voltage).

After separation, proteins were blotted to PVDF membrane in transfer buffer (1 x PAGE buffer with 20 % methanol) with 130 mA current overnight at 4

°C. Western blotting was carried out by blocking the membrane (TBS-T with 5 % milk for PsaB and PsbA antibodies or with 3 % BSA for antiphosphotreonine antibody) for > 1 hour at room temperature or overnight at 4 °C, followed by addition of primary antibodies' solution. For probing PsbA and PsaB we used specific antibodies (Agrisera), and for studying the phosphorylation status of LCHII we used anti-phosphothreonine antibody (Cell Signaling). Additionally, we studied HA-expression in transgenic plants with HA antibody (Roche). After adding the given primary antibody for one to four hours in room temperature or overnight at 4 °C, the membranes were washed six times for five minutes in TBS-T. Secondary antibody for the corresponding animal was added and incubated for 1 hour at room temperature, and then the second wash in TBS-T (6 x 5 min) was carried out. TBS-T was replaced with distilled water, after which chemiluminescence was detected by using Amersham ECL Prime reagents and the BioSpectrum imaging camera (UVP).

4.5.2 Separation of thylakoid protein complexes

We calculated the chlorophyll a and b concentrations by measuring each sample's absorbance at 647 nm and 664 nm. Calculations were done as described by Porra et al. (1989). Thylakoids were isolated as described in Schubert et al. (2002) and separated according to Järvi et al. (2011).

4.6 Statistical analysis and data presentation

Datasets acquired from PAM and OJIP experiments were averaged and normalized in Microsoft Excel 2011 for Mac OS X. We used one-way ANOVA tests with Bonferroni post hoc correction in SPSS program by IBM for statistical analysis (listed in appendices 3-9). Schematic drawings (figure 1 and 3) were drawn by using Procreate for iPad Pro 2017. Final figures were assembled in Microsoft PowerPoint 2011 for Mac OS X.

5 Results

5.1 Generation of *rcd1 ppd8*

A cross between knockout lines *rcd1* and *ppd8* was made in order to investigate whether *PPD8* was the causative gene for the phenotypes of line #28. Firstly, fluorescence kinetics were measured using the imaging PAM (figure 6A). Additionally, visual habitus of the lines was compared (figure 6B).

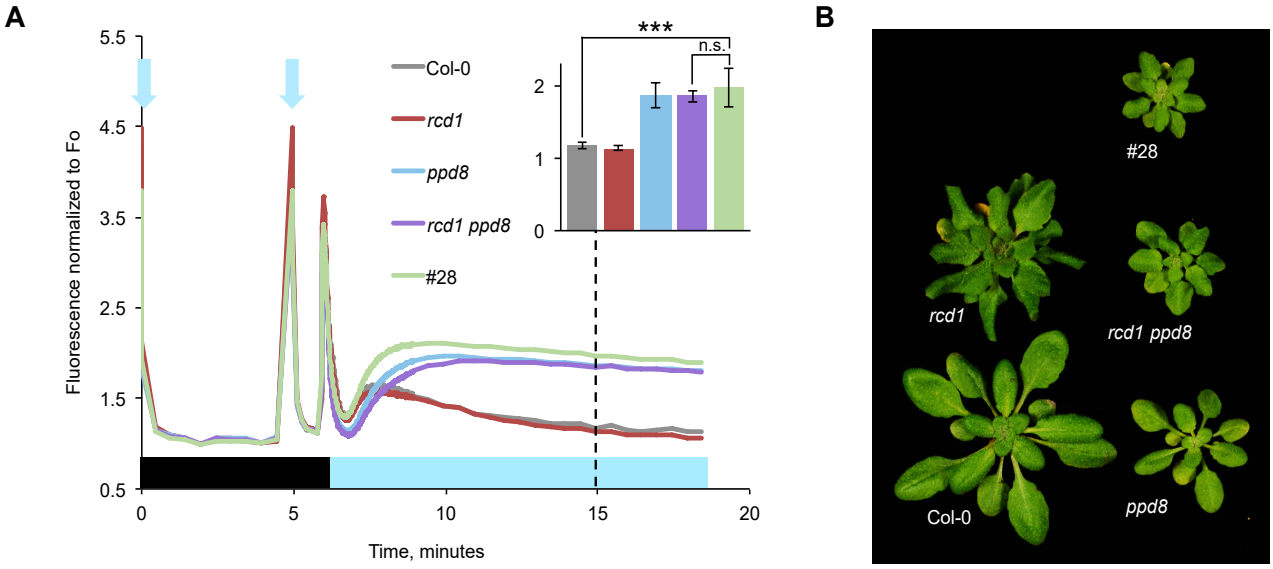

Figure 6. Screen candidate line #28 resembled the double mutant *rcd1 ppd8*. (**A**) PAM kinetics after dark acclimation (black bar) and saturation pulses (blue arrows) show that double mutant *rcd1 ppd8* behaved similarly to #28, being high-fluorescent in light (blue bar) whereas *rcd1* and Col-0 exhibited low fluorescence. Fluorescence values were normalized to minimum fluorescence (Fo) and averaged from four leaf samples. (Inset) the histogram represents the corresponding lines' average fluorescence at 15-minute time point, which is marked with a dashed line. Error bars indicate standard deviations. Three asterisks (***) mark highly significant results ($P < 0.001$) according to one-way ANOVA with Bonferroni post hoc correction, and n.s. stands for non-significant difference (appendix 2). (**B**) A photograph of five-week-old *A. thaliana* lines. Habitus of EMS candidate line #28 was indistinguishable from the double mutant *rcd1 ppd8*.

Figure 6A presents fluorescence kinetics normalized to Fo after dark acclimation. Fluorescence values begun to separate after actinic light was turned on: Col-0 and *rcd1* displayed lower steady-state fluorescence (Fs), whereas #28, *ppd8* and *rcd1 ppd8* had higher Fs. After ten minutes of illumination #28, *ppd8,* and the double mutant displayed almost twice as high fluorescence than WT and *rcd1*. When compared to Col-0, line #28 and *rcd1 ppd8* had statistically

significantly higher fluorescence when measured at 15-minute time point (Figure 6A inset).

Above all, line #28 and *ppd8 rcd1* demonstrated similar high-fluorescence phenotype, and there was no statistical significance between their fluorescence values at 15-minute time point. Furthermore, lines #28 and *rcd1 ppd8* had very similar appearance: their leaves were heavily curled towards ab-axial side like in *rcd1* background plants. They also both had slight yellow color-ation and smaller rosettes. Taken together, the results indicate that *PPD8* is likely the causative gene for the observed phenotypes of line #28, although the definite answer to this question has not yet been given.

5.2 Complementation of *ppd8* and *rcd1 ppd8*

To confirm that the mutation in *PPD8* (At5g27390) gene was causative for the high-fluorescent and MV sensitive phenotypes of *ppd8*, we performed a com-plementation by re-introducing the wild-type copy of the *PPD8* gene to *ppd8* and *rcd1 ppd8* (figure 7).

The T1 individuals expressing the transgene were obtained on antibiotic resistance plates. Following SDS-page protocol (chapter 4.5), we probed with HA-antibody total protein extracts obtained from several of these individuals. Figure 7A shows expression of PPD8-HA in both *ppd8* and *rcd1 ppd8* back-ground plants. Plants of r*cd1 ppd8* background had stronger expression of HA, whereas *ppd8* background plants had much less HA present for an unknown reason. Nevertheless, when rescued lines' phenotypes were observed (figure 7B,C), it was clear that a functional *PPD8* successfully rescued the mutant phe-notypes.

The upper panel of figure 7B shows that *ppd8* was slightly more sensitive to MV than Col-0 at earlier time points: after 5 hours of light the difference be-tween the genotypes was statistically significant ($P < 0.001$). However, no dif-ference was observed at later time points of the light exposure. In contrast, *rcd1 ppd8* was significantly different from *rcd1* during the whole exposure and the dif-ference was growing with time (figure 7B, bottom panel). This indicates that *ppd8* was a true suppressor of the *rcd1*'s tolerance to MV, rather than the muta-

tion that conferred MV sensitivity in any background. In this assay, the rescued *ppd8*:*PPD8-HA* line was indistinguishable from Col-0 (figure 7B, upper panel) while the rescued *rcd1 ppd8:PPD8-HA* performed same as *rcd1* (figure 7B, bottom panel). This strongly supports the idea that *PPD8* is the causative gene responsible for suppressor phenotypes observed in *ppd8* and *rcd1 ppd8*.

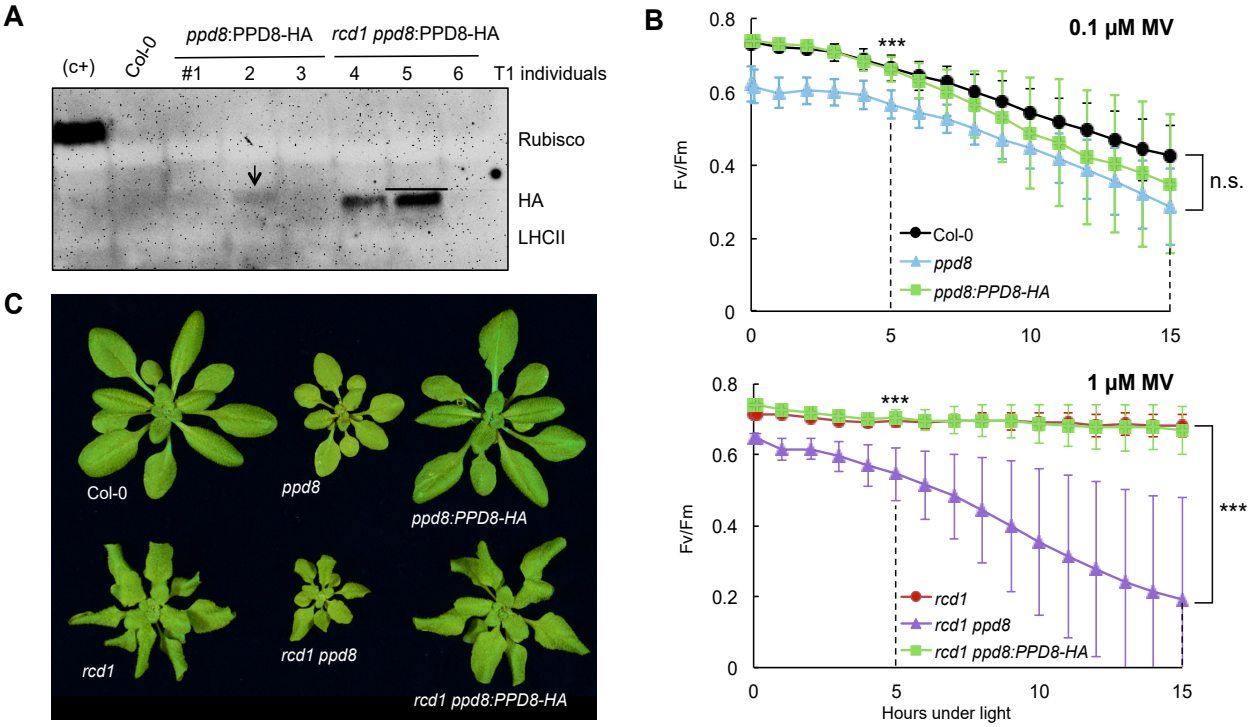

Figure 7. Complementation of *ppd8* and *rcd1 ppd8* by a genetic insertion *PPD8*-HA. (**A**) Expression of HA in several independently complemented *ppd8* and *rcd1 ppd8* plants assessed in T1 generation. Total protein extracts were blotted and probed with HA-antibody. Double mutants expressed more HA than single mutants. (**B**) The rescued lines' tolerance to MV-induced PSII inhibition (Fv/Fm) in presence of 0.1 µM MV (top) or 1 *µ*M MV (bottom) during 15 hours of illumination (80 µmol photons m^{-2} s^{-1}). Data points represent average values from six leaf discs and error bars show standard deviations. Asterisks indicate statistical significance at marked time points: *ppd8* had lower tolerance than *ppd8*:PPD8-HA at five hours whereas the difference was insignificant at 15 hours. In contrast, double mutant *rcd1 ppd8* was significantly less MV-tolerant than either *rcd1* or the rescued line *rcd1 ppd8:*PPD8-HA at both early and late time points. Three asterisks (***) indicate highly significant results ($P < 0.001$) according to one-way ANOVA test with Bonferroni post hoc correction whereas n.s. stands for non-significant difference (appendix 3). (**C**) The habitus of five week old rescued plant lines. WT- or *rcd1*-like phenotype could be restored by *PPD8* gene insertion.

Figure 7C shows the habitus of the generated lines: *ppd8*:PPD8-HA resembled WT (Col-0), while *rcd1 ppd8*:PPD8-HA appeared like *rcd1*. Altogether, these results confirmed that introducing *PPD8* back to knockout-lines reverted their phenotypes back to WT–like and *rcd1* plants. These experiments had two main goals. The first one was to verify that *ppd8* knockout phenotype is indeed caused by the missing *PPD8 gene*. The second goal was to generate PPD8-HA lines for further biochemical studies. For example, to assess the subcellular localization of PPD8-HA. For the first goal, we accomplished to provide evidence for the existence of *PPD8* gene product and its involvement in the studied photosynthetic functions. For the latter goal, more experiments are required to clarify the localization of PPD8 protein *in planta*.

5.3 Defects in NPQ

Line #28 displayed sensitivity to MV in the preliminary studies (figure 4B). Additionally, double mutant *rcd1 ppd8* was high-fluorescent, as seen in figure 6A and sensitive to MV (figure 7B). To study whether these high fluorescence phenotypes were paralleled with changes in NPQ, we applied two methods to evaluate the NPQ in *ppd8* background: PAM and OJIP (figure 8). Treatment of plants with MV leads to increased NPQ (Shapiguzov et al, 2020). Thus, the effect of MV on NPQ was also measured in *ppd8*.

We used PAM imaging (protocol in methods 4.4.1) to calculate average NPQ ((Fm-Fm')/Fm', according to Baker, 2008) of Col-0, *ppd8*, *rcd1* and *rcd1 ppd8* from four leaf discs during one hour of non-saturating actinic light exposure (80 µmol photons m^{-2} sec^{-1}) after dark acclimation (figure 8A).

Unexpectedly, *ppd8* exhibited significantly higher NPQ than Col-0. Interestingly, in this assay the development of NPQ in the mutant *rcd1 ppd8* was similar to *rcd1* as well as to WT: tested with one-way ANOVA these differences were insignificant whereas only single mutant *ppd8* had significantly more elevated NPQ. This suggests that *rcd1* mutation to suppressed the high NPQ phenotype of *ppd8*.

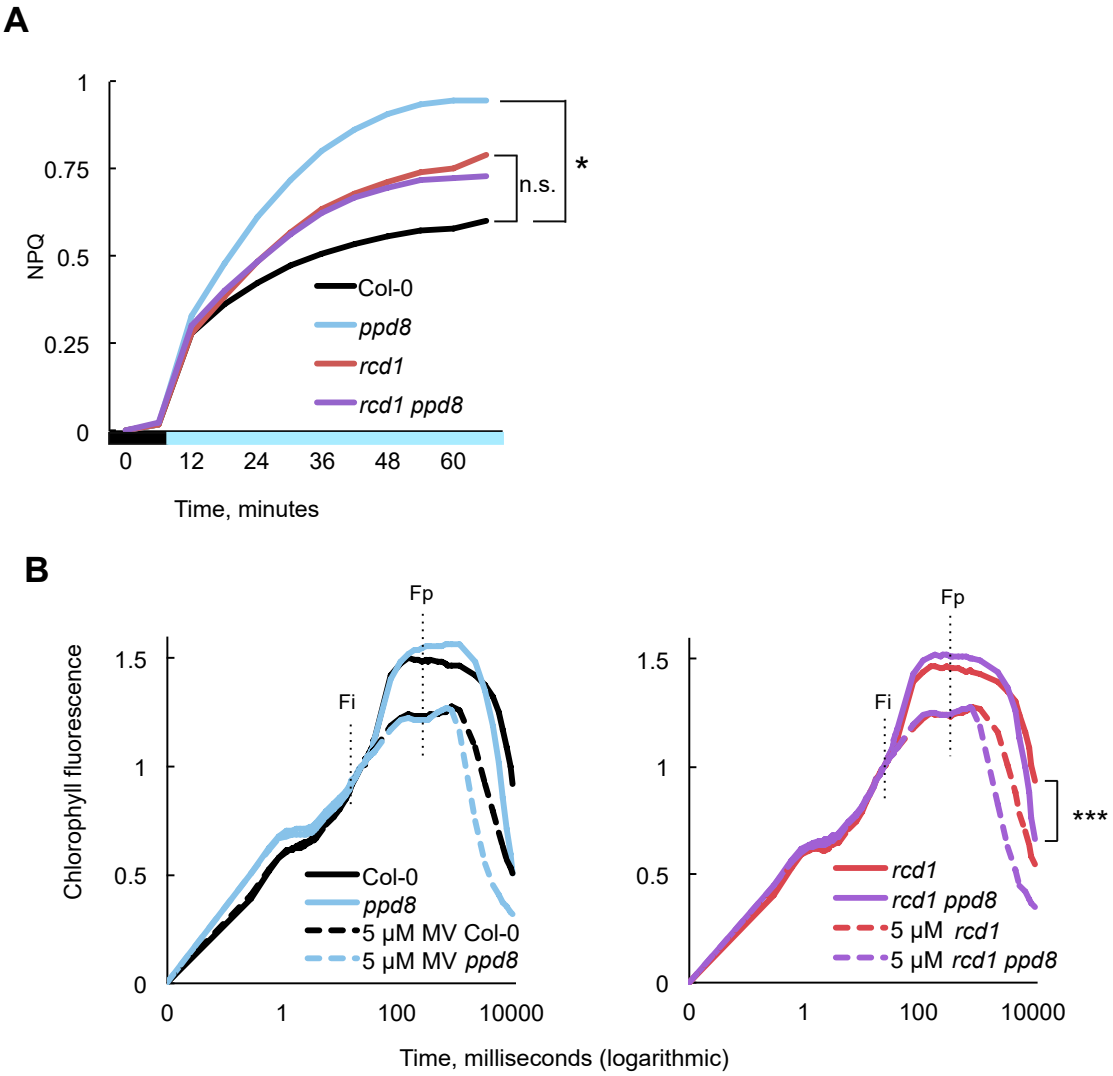

Figure 8. NPQ was more pronounced in *ppd8* mutant. (**A**) Average NPQ estimates from four leaf discs in light (blue bar) after darkness (black bar). After an hour of illumination (80 µmol photons m^{-2} s^{-1}) only *ppd8* had significantly higher NPQ than Col-0. One asterisk (*) indicates statistical significance ($P < 0.05$) according to one-way ANOVA with Bonferroni post hoc correction, and n.s. stands for non-significant results (appendix 4). (**B**) OJIP kinetics of single *ppd8* (left panel) and double *rcd1 ppd8* mutants (right panel). Dashed curves depict fluorescence in presence of 5 *µ*M MV. Values were double normalized to Fo (at 20 *µ*s) and Fi (at 25 ms). Values after Fi display the impact of MV downstream from PSI electron transfer. The decrease of fluorescence after Fp phase is correlated with lumen acidification and NPQ, especially with its qE component. Faster relaxation of fluorescence after Fp peak can be observer in *ppd8* mutant in presence of MV and without it. OJIP kinetics were more similar between *rcd1 ppd8* and *rcd1*, but also here the more rapid decrease after Fp is present. At 10800 ms time point the difference in fluorescence between *rcd1* and *rcd1 ppd8* was highly significant (*** $P < 0.001$) according to one-way ANOVA with Bonferroni post hoc correction, indicating higher NPQ in the double mutant (appendix 5).

As a complementary approach we performed OJIP measurements in the corresponding lines (figure 8B). All leaf discs were dark adapted for one hour with or without 5 μM MV. Then the plant material was illuminated with the 12-second flash of strong light (> 3 000 µmol photons m^{-2} sec^{-1}) and chlorophyll fluorescence was recorded and plotted against time on logarithmic axis. OJIP kinetics were double normalized to Fo and Fi in order to show more clearly the effect of MV on PSI electron flow. As described in chapter 1.3, NPQ, especially its qE element is associated with the decrease in fluorescence after Fp peak in OJIP kinetics (Demmig-Adams, 1990). When we compared *ppd8* to Col-0 and *rcd1 ppd8* to *rcd1*, more rapid relaxation in fluorescence could be observed in the mutants with *ppd8* background at Fp or after it, both with and without MV. Because MV catalyzes electron transfer from PSI to oxygen, Fi-Fp-phase of the OJIP transient is lower when MV is present. In each case, *ppd8* background mutants had lower fluorescence after Fp peak, which agreed well with higher NPQ in *ppd8*. It is worth a note that both in PAM-based and OJIP-based estimations of NPQ the difference between *ppd8* and Col-0 were higher than the difference between *rcd1 ppd8* and *rcd1*. This suggests that the *rcd1* mutation is to some extent suppressing the defects of photosynthesis and NPQ observed in *ppd8*.

5.4 Photosynthetic phenotypes of *ppd8*

Several observations seen in *ppd8* suggested that the photosynthetic apparatus was affected. Firstly, *ppd8* had a habitus that was less green and smaller when compared to Col-0 (figure 6B). Its chlorophyll fluorescence and sensitivity to MV were higher than those of Col-0 (figure 6A and figure 7B). Finally, the elevated NPQ (figure 8A) and the altered OJIP-transient (figure 8B) in *ppd8* background plants hinted towards disturbances in the electron flows. Taken together, these results implied that the photosynthetic machinery is impaired in *ppd8*. To study this possibility in detail, we assessed biochemically the status of photosynthetic proteins in *ppd8* (figure 9A, B).

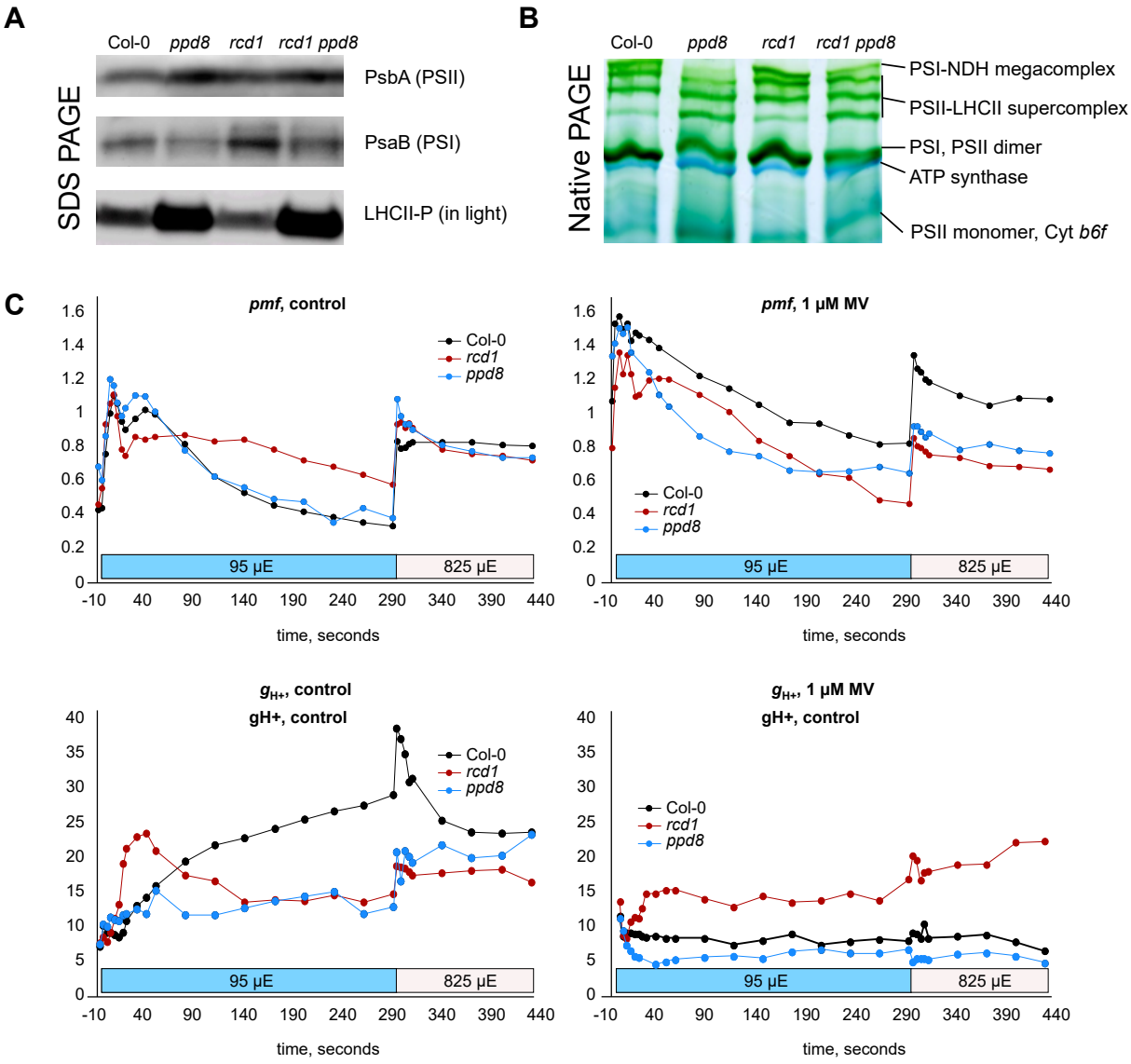

Figure 9. Photosynthetic phenotypes of *ppd8* mutants. (**A**) Protein extracts from dark-adapted plants were separated by SDS-page and immunoblotted with anti-PsbA, -PsbA, or -phosphothreonine antibodies. Total amount of PsbA was larger in *ppd8* background plants, whereas PsaB was accumulating at lower amounts. LHCII was more phosphorylated in *ppd8* background, which may have been an attempt of plants to compensate disrupted PSII/PSI stoichiometry. (**B**) Native PAGE of solubilized thylakoids also exhibit lower amounts of PSI-NDH megacomplex in *ppd8*. Intriguingly, ATP synthase appeared to be more abundant in *ppd8*. Thylakoid assay is interpreted as in Järvi et al., 2011. (**C**) *Pmf* and conductivity of the thylakoid membrane to protons (g_{H+}) were measured via the electrochromic pigment absorbance shift (ECS) in water (left panels) and in 1 μM MV (right panels). The blue bar represents low light intensity and the white bar indicates high light intensity. *Pmf* was lower in *ppd8* and Col-0 when compared to *rcd1* in water under low light conditions. In high light *pmf* was more similar between *ppd8* and *rcd1*. Interestingly, MV did not heavily affect *pmf* in *ppd8*. The bottom panel represents g_{H+} without MV (bottom left panel) and in 1 μM MV. *Ppd8* has higher conductivity in high light without MV than *rcd1*, whereas in the presence of MV the conductivity decreases even lower than WT. These measurements were provided by our collaborator Lauri Nikkanen (University of Turku).

Figure 9A features immunoblotting results from total protein extracts of Col-0, *rcd1*, *ppd8*, and *rcd1 ppd8*. Protein extracts were tested with PsbA, PsaB and anti-phosphothreonine antibodies revealing the amount of PSII, PSI, and the phosphorylation status of LHCII, accordingly. PsbA, the core subunit of PSII, was more abundant in *ppd8* compared to WT and in *rcd1 ppd8* in comparison to *rcd1*. The amount of PSI core protein PsaB was lower in *ppd8* and *rcd1 ppd8*. Photosystems obey strict stoichiometry rules, which means that by looking at abundance of their individual component proteins one can infer the relative abundance of the whole photosystem. Thus, these results suggest that the absence of *PPD8* resulted in higher accumulation of PSII and lower accumulation of PSI, leading to an unbalanced stoichiometry of PSII/PSI in *ppd8* plants.

We also examined the phosphorylation status of LHCII to study the activity of state transitions. The bottom row in figure 9A presents that LHCII was more phosphorylated in *ppd8* suggesting that it was more functionally connected to PSI than to PSII. This data is consistent with high fluorescence and unbalanced PSII/PSI stoichiometry: *ppd8* may attempt to compensate the lowered amount of PSI by associating more LHCII to it. As explained in chapter 1.2.1, plants use LHCII state transitions to redistribute excitation energy between PSII and PSI in fluctuating light conditions.

In addition to LHCII phoshorylation status, we desired to inspect the amount of large thylakoid protein complexes, i.e mega- and supercomplexes. For this, we have isolated thylakoids from dark-adapted plants. Figure 9B presents a native PAGE assay on which O/N dark-adapted Col-0, *ppd8*, *rcd1* and *rcd1 ppd8* thylakoid isolates were separated. The photosynthetic complexes are interpreted according to Järvi et al. 2011 and Aro et al. 2005. The uppermost band is the PSI-NDH megacomplex – a large multiprotein complex that is involved in cyclic electron flow (CEF). In comparison to Col-0, *ppd8* had a lower amount of PSI-NDH, which is consistent with our previous observation of *ppd8*'s compromised PSI accumulation. P-LHCII has been linked to formation of PSI-Cyt b_6f complex and therefore to activation of CEF (Iwai et al. 2010). It is thus possible that high phosphorylation of LHCII observed in Fig 9A is a compensatory adaptation of a plant to its deficiency in forming the PSI-NDH mega-

complex. Clarification of this regulation requires further studies, as plants can perform CEF via several mechanisms, as described in chapter 1.2.2.

Interestingly, the amount of ATP synthase was elevated in *ppd8* background plants. To test whether altered ATP synthase abundance was paralleled by its changed function, we measured pmf in *ppd8* plants. A pilot experiment was conducted in collaboration with Dr. Lauri Nikkanen at the University of Turku (figure 9C). *Pmf* and g_{H+} were measured under two different light intensities via the electromagnetic pigment absorbance shift (ECS). Prior studies have shown that ATP synthase activity is suppressed by MV (Shapiguzov et al, 2020). Thus, we performed our measurements in water control conditions or in presence of MV. *Ppd8* demonstrated similar *pmf* to WT in lower light intensity without MV. However, pmf of *ppd8* was lower in high light and in the presence of MV. This lowered *pmf* of *ppd8* in low light could be linked to the elevated amount of ATP synthase observed in native PAGE or to decreased photosynthetic efficiency. Proton conductivity of the thylakoid, however, was lower in *ppd8* than in WT in both high and low light intensities. As g_{H+} reflects more directly the activity of ATP synthase (Kanazawa and Kramer, 2002), it is possible that ATP synthase is misfolded and/or functioning improperly in *ppd8.* It is worth noting that these pilot measurements were made in 1-2 replicates, thus any conclusions about the ATP synthase activity in *ppd8* requires further experiments. Overall, the biochemical and spectroscopic analyses revealed defects in abundance of Photosystems, of the NDH-containing supercomplexes and of ATP synthase. NDH complex and ATP synthase are the two main complexes establishing the transthylakoids protin gradient (figure 1). So, the defects in their activities and / or accumulation could be the molecular basis for the observed defects in NPQ (figure 8).

5.5 Phenotypes of *rcd1 ppd8 ntrc*

Activity of chloroplastic ATP synthase is regulated through Trx systems (Ketcham et al. 1984, Hangarter et al. 1987, Junesch and Gräber, 1987). Recently, thiol regulatory enzyme NTRC was proposed to have an essential role in the regulation of ATP synthase – specifically under low light conditions (Nik-

kanen et al. 2016, Carrillo et al. 2016). Shapiguzov et al. (2020) revealed that both activity of CEF and ATP synthase depend on NTRC. Furthermore, NTRC was suggested to contribute to regulation of photosynthetic electron transport in *rcd1*. Because *ppd8* was discovered in rcd1 suppressor screen and because this mutant exhibited defects related to the two targets of NTRC, ATP synthase and NDH, we next asked how is NTRC-related regulation linked to PPD8 functions. Thus, we made a cross between *rcd1 ppd8* and *rcd1 ntrc* and generated the triple *rcd1 ppd8 ntrc* mutant (figure 10).

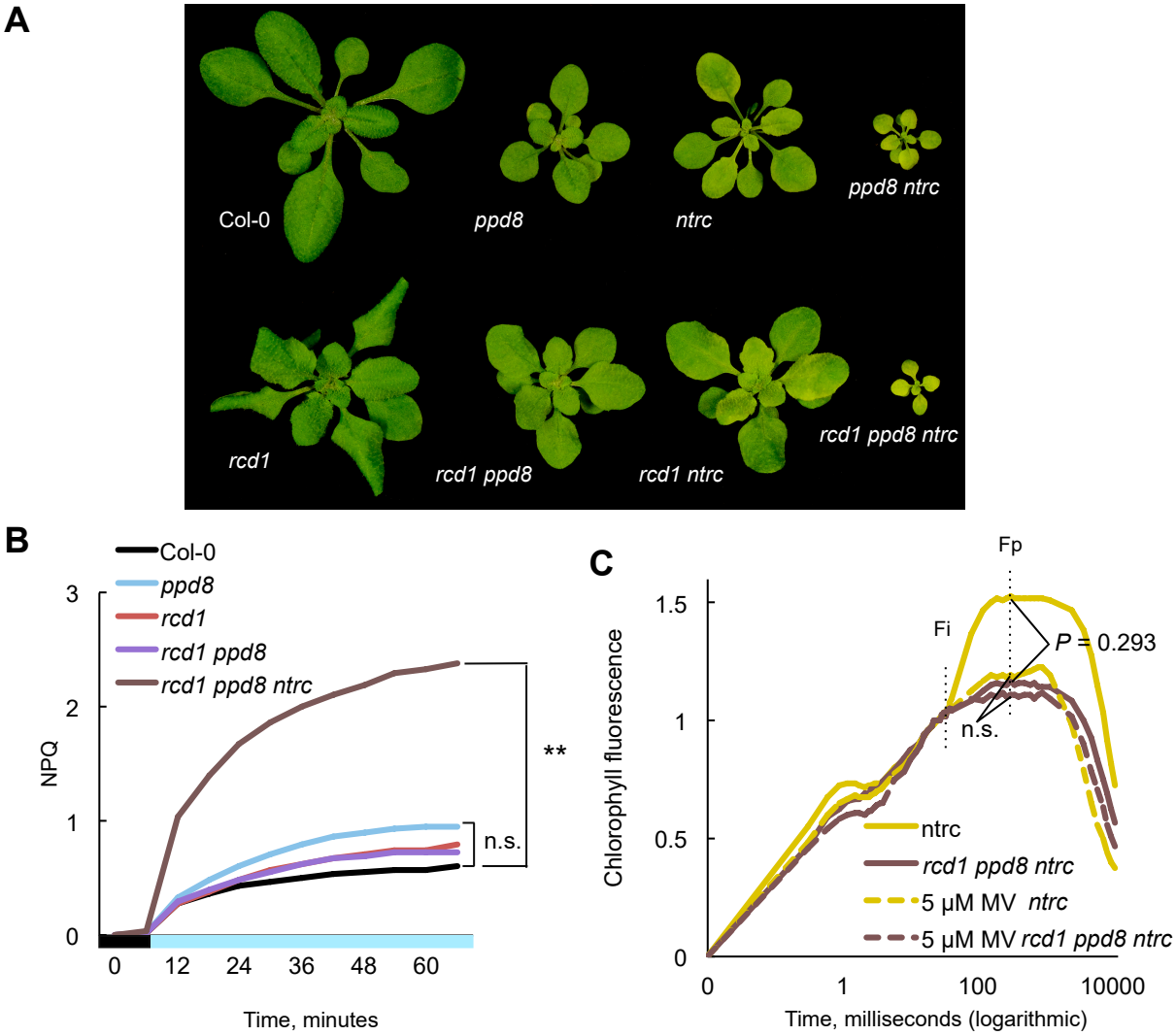

Figure 10. Knocking out *NTRC* affects strikingly the phenotypes of plants. (**A**) Habitus of 2,5-week old knockout lines. Both *ppd8 ntrc* and *rcd1 ppd8 ntrc* demonstrated profoundly compromised growth. (**B**) Averaged NPQ estimates from four leaf discs, calculated according to Baker, 2008. After one hour of light (80 µmol photons m^{-2} s^{-1}, blue bar) triple mutants displayed over two times higher NPQ when compared to Col-0 whereas other lines' estimates were non-significant (marked with n.s.). Two asterisks (**) stand for $P < 0.01$ according to one-way ANOVA test with Bonferroni post hoc correction (appendix 6). (**C**) OJIP transients of *ntrc* and *rcd1 ppd8 ntrc*. The effect of 5 µM

MV is presented with dashed lines and fluorescence values were double normalized to Fo and Fi. Of note is the effect of MV in the triple mutant: the fluorescence of Fi-Fp-phase remained flat. When *ntrc* and the triple mutant were compared either with or without MV at Fp, the values weren't significantly different according to one-way ANOVA with Bonferroni post hoc correction (appendix 7).

Figure 10A presents phenotypes for all knockout mutants used in this study. In comparison to other knockout plants the double mutant *ppd8 ntrc* and the triple mutant *rcd1 ppd8 ntrc* were very compromised: they had minuscule, pale leaves and their flowering times were extremely delayed. We examined the triple mutant's NPQ via PAM and OJIP. Figure 10B presents NPQ calculations acquired from PAM during 60 min of illumination according to protocol in chapter 4.2.1. The triple mutant displayed over two times higher average NPQ than other mutant lines. OJIP imaging also revealed faster rate of fluorescence decrease after Fp (i.e., higher NPQ) in *rcd1 ppd8 ntrc* when compared to the single *ntrc* mutant (figure 10C).

Strikingly, in the *rcd1 ppd8 ntrc* triple mutant the effect of MV on electron transfer downstream from PSI was largely abolished, as the kinetics with and without MV resembled each other (figure 10C), whereas the double mutant *rcd1 ppd8* was more affected by MV (figure 8B). These anomalies in Fi-Fp-phase of *rcd1 ppd8 ntrc* and irresponsiveness of this phase to MV treatment suggested that knockout of both *ppd8* and *ntrc* significantly altered electron transfer downstream from PSI and, possibly, to some extent mimicked the damaging effect of MV on photosynthesis.

5.6 PPD8 is not related to mitochondrial functions of *rcd1* and is partially redundant with NTRC

Rcd1 was discovered to have an altered phenotype in hypoxia that is hypothetically linked to mitochondrial respiration (Shapiguzov et al. 2020). The effect of MV on OJIP disappears under hypoxic treatment in the *rcd1* mutant, but not in Col-0. In order to see if *ppd8* affects *rcd1* phenotypes that are supposedly linked to mitochondrial activities and aerobic respiration, we performed OJIP measurements under hypoxic conditions induced by adding nitrogen gas to the testing chamber (figure 11).

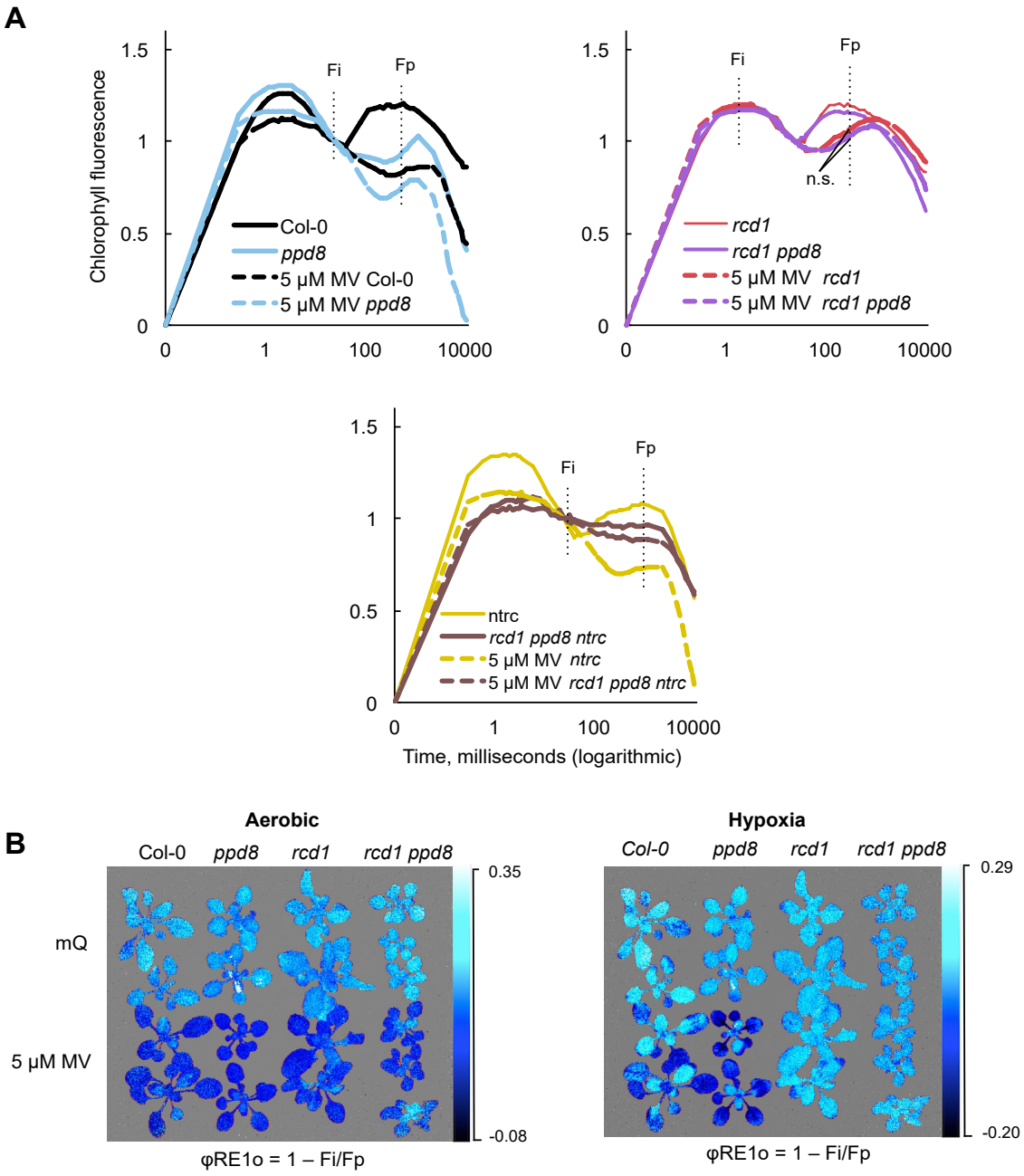

Figure 11. *Ppd8* mutation did not suppress the hypoxic fluorescence phenotypes of *rcd1*. (**A**) OJIP transients in hypoxic conditions. The OJIP kinetics under 5 μM MV is presented with dashed lines. The fluorescence values were averaged from four leaf discs (three for *rcd1 ppd8 ntrc*) and double normalized to Fo (at 20 μs) and Fi (at 25 ms), which is marked with a dashed vertical line. If *ppd8* had suppressed the mitochondrial phenotypes of *rcd1* observed by Shapiguzov et al. (2020) the double mutants' OJIP kinetics would have resembled more the fluorescence of Col-0, which is not the case. Instead, when Fp is observed under the influence of MV, the difference between *rcd1* and *rcd1 ppd8* is n.s. according to one-way ANOVA test with Bonferroni post hoc correction (appendix 8). (**B**) False-colour image of the quantum yield of the electron transport flux until the PSI electron acceptors, calculated as ϕRE1o = 1 – Fi/Fp. Plants were treated with or without 5 μM MV and then subjected to aerobic or hypoxic conditions. The effect of MV on the Fi-Fp-phase is absent in *rcd1* background plants, with *rcd1 ppd8* being indistinguishable from *rcd1*.

Hypoxic OJIP transients are presented in figure 11A: kinetics are averaged measurements from four samples that were treated with 5 μM MV or water control. The left panel presents *ppd8* compared to Col-0. The middle panel shows *rcd1 ppd8* compared to *rcd1* and the right panel presents results for the triple mutant compared to *ntrc*. Unlike OJIP in aerobic conditions (figure 8B), under hypoxia the response of MV-pretreated and control plants is very similar in *rcd1*. Furthermore, the middle panel reveals that *rcd1 ppd8* resembled more *rcd1* than WT. This suggests that *ppd8* is not the suppressor of this hypothetically mitochondria-related phenotype of *rcd1* since the double mutant had similar OJIP transient to *rcd1* under MV.

Figure 11B shows false colour images of ϕRE1o = 1 – Fi/Fp values in plant rosettes after one hour treatment with or without 5 μM MV. ϕRE1o represents the Fi-Fp-phase: it has been linked to the quantum yield of the electron flux to PSI side electron acceptors (Schansker et al. 2005). Here, the effect of MV was diminished in *rcd1* and double mutant *rcd1 ppd8*. In hypoxia, the double mutant displayed similar ϕRE1o values to *rcd1* i.e. *ppd8* had no effect on the mitochondrial phenotype of *rcd1*.

Interestingly, spatial heterogeneity of rosettes observed under imaging OJIP suggests that response to combined effect of hypoxia and MV varied between the leaves of different age. This could indicate developmental difference in plant hypoxia response. Novel imaging OJIP shows potential for studying photosynthesis in different plant tissues and plant material at various developmental stages.

Both in aerobic and hypoxic environment, MV had only a slight effect on the triple mutant's fluorescence (figure 10C and figure 11A, right panel, accordingly). In both cases, the Fi-Fp-phase of the curve remained flat both in MV-treated and control conditions. This indicated significant alterations of electron transfer pathways downstream from PSI in the triple mutant. Thus, knockout of both *ppd8* and *ntrc* has severely affected photosynthesis. This is in line with the stunted habitus of the *ppd8 ntrc* and *rcd1 ppd8 ntrc* plants. This also suggests that *ppd8* and *ntrc* play partially redundant functions in the regulation of photosynthetic apparatus.

6 Discussion

PPD8 is one of many photosynthesis-associated genes, the functions of which are yet to be explored: there are no previous experimental attempts to characterize PPD8 protein or its relevance for photosynthetic performance. We chose to study *ppd8* knockout *A. thaliana* plants based on the results acquired from a preceding *rcd1* suppressor screen. The screen was conducted on *rcd1* background plants with intent to search for candidate genes that could revert MV resistance phenotype of *rcd1*. Promising candidate lines were sequenced, from which line #28 showed a genetic disruption in the locus AT5G27390, later addressed as *PPD8*.

Ongoing studies in our lab have suggested several possible non-mutually exclusive explanations of the MV resistance of *rcd1*. One line of evidence hinted that MV tolerance of *rcd1* is associated with distorted thiol redox states of chloroplast redox enzymes, including NTRC. This enzyme regulates both ROS metabolism and activity of several key photosynthetic complexes, ATP synthase and NDH complex among them (Nikkanen et al. 2016). Another line of evidence implies that MV tolerance of *rcd1* might arise from altered electron transfer downstream from PSI. Interestingly, we hypothesized that oxygen availability may be lowered in the *rcd1* chloroplasts, which could consequently affect both ROS formation and photosynthetic electron transfer (Shapiguzov et al, 2020). From this standpoint we pursued to investigate the function of PPD8 by using both a single *ppd8* mutant and a double mutant *rcd1 ppd8.* We addressed the roles of *PPD8* in the context of light responses, MV response and photosynthetic performance. Additionally, we studied the interactions of PPD8 with NTRC.

First, it was necessary to study whether the phenotypes in line #28 were indeed determined by the loss of function of *PPD8.* We approached this research question by crossing an independent T-DNA allele of *ppd8* with *rcd1* and comparing the phenotypes of *rcd1 ppd8* to those of line #28. The *rcd1 ppd8* mutant demonstrated similar habitus and photosynthetic phenotypes as the candidate line #28. This supported our hypothesis that *PPD8* was the causative gene responsible for the suppressor phenotypes observed in the line #28 (figure 4).

To directly prove that the observed phenotypes of *ppd8* and *rcd1 ppd8* were caused by the disruption of the *PPD8* gene, we tagged the *PPD8* gene with C-terminal HA tag and re-introduced it to *ppd8* and *rcd1 ppd8* knockout mutants. In the generated *ppd8*:PPD8-HA lines the habitus and the MV tolerance was reverted to wild-type. In the *rcd1 ppd8*: PPD8-HA lines the habitus and the MV tolerance was similar to that of *rcd1*. We confirmed the presence of PPD8-HA insertions by immunological assays. Taken together, these experiments strongly supported the idea that *PPD8* was the causative gene implicated in MV tolerance of the *rcd1* mutant.

Importantly, while MV resistance and PSII efficiency of *ppd8* was similar to that of Col-0, the MV tolerance of *rcd1 ppd8* was substantially lower than that of *rcd1* (figure 5). This indicated that *PPD8* is the true suppressor of *rcd1*, i.e., it is directly involved in the MV tolerance of the *rcd1* mutant.

The loss of *PPD8* gene resulted in altered photosynthetic phenotypes. Both *ppd8* and *rcd1 ppd8* displayed elevated amounts of PSII core subunit PsbA but decreased amount of PSI subunit PsaB, as we determined by SDS-PAGE and Western blotting. Furthermore, altered stoichiometry of photosynthetic complexes was observed by native PAGE technique, which allows visualization of large thylakoid protein-pigment complexes. Our preliminary results indicate that plants lacking *PPD8* accumulated more PSII monomers and PSII-LHCII-supercomplexes, more ATP synthase but less PSI-NDH megacomplexes. PPD8 has previously been suggested to function as an auxiliary protein involved in stabilization and / or assembly of photosynthetic complexes, although the exact targets were unclear (Sato, 2010; Järvi et al., 2013). Our results indicate that PSII and PSI may be among the targets of PPD8.

A possible functional outcome of the PSI / PSII stoichiometric imbalance is the altered redox state of the PQ pool. We addressed PQ redox state indirectly, by measuring phosphorylation status of LHCII in *ppd8* and *rcd1 ppd8*. This is possible because the LHCII kinase STN7 is activated by more reduced PQ (Vener et al., 1997; Zito et al., 1999). The levels of P-LHCII were elevated in *ppd8*, suggesting that the PQ pool was likely more reduced. This observation is in line with higher PSII and lower PSI activity in this mutant. Because P-LHCII

has higher affinity to PSI than to PSII (Allen & Forsberg 2001, Grieco et al. 2015), it is possible that higher phosphorylation of LHCII antennae helps *ppd8* to compensate the imbalanced stoichiometry of photosystems via promoting PSI light harvesting. Another characteristic feature of *ppd8* was the increased NPQ. We measured NPQ in *ppd8* plants via two methods: PAM and OJIP. Both results showed that *ppd8* plants had elevated NPQ when compared to WT and *rcd1* (figure 10).

The question remained open how could PPD8 contribute to MV tolerance of the *rcd1* mutant. The ongoing research in our lab has linked this phenotype of *rcd1* to altered activity of chloroplast ATP synthase and NDH complex. Both of these complexes participate in formation of trans-thylakoid proton gradient, thus affecting NPQ. Importantly, abundance of both of these complexes has been altered in *ppd8*, as seen in the native PAGE gels (figure 9). Moreover, the ECS measurements revealed that whereas the function of the chloroplast ATP synthase was unchanged in *ppd8* under control conditions, treatment of plants with MV resulted in different *pmf* response in *ppd8* and Col-0 (figure 9C). Taking the above facts in consideration, we conclude that the implication of PPD8 in MV tolerance may be related to the function of chloroplast ATP synthase and NDH complex. Further research is needed to provide mechanistic understanding of how PPD8 regulates these photosynthetic complexes. In the future, we plan to use the generated PPD8-HA lines to define in which sub-plastidial localization PPD8 resides. This is possible by isolating and fractioning chloroplast envelope membranes, stroma, and thylakoids, together with further analysis by immunoblotting and/or mass spectrometry based proteomics.

NTRC is known to contribute to the regulation of ATP synthase and NDH complex (Nikkanen et al. 2016, 2017; Carrillo et al. 2016). This thiol enzyme has also been studied in the context of nuclear regulator RCD1 (Shapiguzov et al. 2020). To address genetic interaction of PPD8 and NTRC, we generated the double mutant *ppd8 ntrc* and the tipple mutant *rcd1 ppd8 ntrc*. These mutants were characterized by compromised photosynthetic efficiency and markedly retarded growth. They also had profoundly increased NPQ. This strikingly elevated NPQ could indicate further dramatic decrease in the activity of the ATP-

synthase. Additionally, we saw that the triple mutant behaved in a peculiar manner when MV is introduced: the electron transfer downstream from PSI was largely abolished in OJIP measurements for an unknown reason. Finding the reasons for this are the subject of futher research. Overall, these results suggest that both PPD8 and NTRC are involved in the regulation of trans-thylakoid proton gradient. The severe phenotype of the double *ppd8 ntrc* knockout hinted that this regulation occurs in two independent but complementary ways.

The absence of PPD8 altered the chloroplastic phenotypes of *rcd1,* manifested as high fluorescence, decreased MV tolerance and altered protein levels. Thus, we wanted to examine if *rcd1 ppd8* had changes in the mitochondrial phenotypes as well. In hypoxic conditions *rcd1 ppd8* had very similar OJIP fluorescence kinetics as compared to *rcd1*. If *ppd8* was also a suppressor of *rcd1* mitochondrial phenotypes observed in (Shapiguzov et al. 2020), the fluorescence would have resembled the WT's which was not the case. Instead, the hypoxic OJIP kinetics were similar to those of *rcd1.* From this we conclude that *ppd8* is suppressing chloroplastic, but not mitochondrial phenotypes of *rcd1.*

The preliminary design for our study differed to some extent from the final experiments we ultimately performed. For example, the initial aim was to confirm the causative gene for the suppression screen. The screen itself was carried out before this project; therefore limited information about this process was described in this thesis. While we verified that *PPD8* was the causative gene for the high light sensitivity and high fluorescence in line #28 we didn't carry out tests comparing MV tolerance between different lines. It is tempting to assume that *rcd1 ppd8* is the corresponding genotype responsible for the poor MV resistance in #28, yet we don't have direct comparison but only analogous measurements that seem to provide similar fluorescence kinetics. To directly prove that PPD8 was the causative gene for the phenotypes observed in line #28 one has to perform the allelism test. However, this experiment has not yet been done. It is worth noticing, that the main goal for this thesis wasn't the study of a screen candidate line, but instead it was to study *ppd8* in relation with *rcd1*.

Retrospectively, some experiments could have complemented this study beneficially. Ideally, we could have studied the photosynthetic phenotypes and

efficiency of *ppd8 ntrc* double mutants; however, these plants were extremely difficult to propagate due to their poor growth.

This study was an attempt to decipher the relations of one unknown gene with the help of other genes. Nothing but vague predictions was known about the function of *PPD8*, which provided challenges but on the other hand also many possibilities for experimenting. The putative roles for this gene were only suggestions based on distant gene homologies from animal kingdom and functional predictions established on amino acid sequence. According to The Arabidopsis Information Resource (TAIR), some suggested roles for PPD8 were e.g chloroplastic tagatose isomerase, PSII auxiliary protein and/or association to ribosomal functions. We provided evidence that PPD8 is necessary for correct functioning of photosynthesis and the stoichiometry of photosystems. Moreover, our results propose that the lack of PPD8 may lead to excessive acidification of lumen, thus leading to our observed phenotypes of *ppd8*: increased amount of phosphorylated LHCII, high chlorophyll fluorescence and elevated NPQ. The decreased lumenal pH observed in *ppd8* is likely due to the imbalance in stoichiometry of photosystems, ATP synthase and/or NDH complexes. However, other secondary effects are also possible, i.e. incorrect spatial organization of thylakoid membranes and photosynthetic machinery. There are many potential future experiments to gain better understanding of PPD8 function. For example, microscopy would be a promising tool for assessing whether knockout lines have altered structure in chloroplast thylakoid membranes or plastid morphology altogether.

In addition to microscopy, other possible future experiments could be the previously mentioned chloroplast compartment fractionation and immunoblotting for HA in our complemented lines, e.g. by following protocol provided by Bouchnak et al. 2018. Furthermore, the activity of ATP-synthase could provide more detailed insight on the *ppd8* mutant. This could be tested with proton motive force measurements as described by Nikkanen et al. 2018, and/or by immunoblotting with corresponding ATP-synthase antibody. We could also acquire more detailed information about PPD8 through protein isolation and X-ray crystallography as well as computational modelling with bioinformatic tools. In order

to search for different domains and predicted protein activity it is possible to use available online databases. However, this approach requires complementary evidence from experimenting. Other alternative experiments could have been related to the overexpression of *PPD8*. However, the time window allowed us to generate only one complementation line with the native *PPD8* promoter.

The complete picture of light reactions remains unclear despite the knowledge on how photosynthesis acts as the basis of terrestrial biodiversity and a major contributor to humanity's nutrition, medicine, energy production and infrastructure. It is crucial to map each gene contributing to the photosynthetic machinery and its regulators in order to understand and potentially modify photosynthesis for better agricultural yield and energy production. It appears challenging to fully comprehend photosynthesis as a whole since plants have large genomes and their capacity to acclimate takes account of an innumerable amount of environmental and developmental parameters. However, the ever-increasing efficiency of computational power can act as the leading force for growing biological knowledge in the near future. Thus, the combination of experimental research like this study and bioinformatic tools will be the key for understanding plant life.

7 Conclusions

PPD8 gene product was confirmed in model organism *Arabidopsis thaliana*. In this thesis, evidence for the importance of PPD8 in photosynthesis is provided. PPD8 is an auxiliary protein that is required for optimal photosynthesis based on the following observations:

1. Plants lacking a functional *PPD8* gene are sensitivie to high light and display high chlorophyll fluorescence as well as high levels of non-photochemical quenching.

2. Without PPD8, the stoichiometry of photosystems is unbalanced. Additionally, *ppd8* plants have higher levels of phosphorylated LHCII, increased abundance of ATP synthase supercomplex and possibly decreased abundance of PSI-NDH megacomplex.

3. When the nuclear protein RCD1 is absent in *A. thaliana*, plants are tolerant to chloroplastic ROS accumulation. This tolerance can be partially suppressed by knocking out *PPD8*. Thus, *PPD8* affects ROS processing in chloroplasts.

The precise functions of PPD8 and mechanisms in which PPD8 affects to the operation of photosynthesis are not known. However, it is evident that small auxiliary proteins are crucial when trying to understand the photosynthesis as a whole.

8 Acknowledgements

I'd like to give my thanks to the evaluators who kindly agreed to grade my thesis in a shorter time frame than usual, as well as to the programme director for his help and quick responses. Even during these exceptional times the communication worked and things got arranged without any complications.

Thanks for the Kangasjärvi research group for providing resources for this study and also for the helpful people who assisted me in the lab. Additional credit goes to our collaborator Lauri Nikkanen, who contributed to this thesis by executing interesting pivotal ECS experiments.

Most importantly, I want to give my thanks to my brilliant supervisor Alexey. I honestly think that if I chose any other thesis subject than this project, I could've not finished it. Thank you for your patience, excellent pedagogical touch and direction during the whole time from the lab work to the revision of the text. I appreciate your visions, both scientific and artistic. Instead of being overly exhausted or already fed up with research field during this long project, I'm feeling inspired and ever more intrigued about the plant world.

I'm extremely grateful for the support I received at home: thank you Konsta for being cheerful even on a rainy day and believing in me when I didn't. I'm also thankful for the company provided by my friends – study related or not. I want to thank my parents and family for a life-long encouragement and reassurance that carries me on every day. Big extra thanks goes to my little friend Coco who eased my stress like nothing else.

9 References

Albertsson, P. Å. (2001). A quantitative model of the domain structure of the photosynthetic membrane. *Trends in plant science*, *6*(8), 349-354.

Andersson, B., & Anderson, J. M. (1980). Lateral heterogeneity in the distribution of chlorophyll-protein complexes of the thylakoid membranes of spinach chloroplasts. *Biochimica et Biophysica Acta (BBA)-Bioenergetics*, *593*(2), 427-440.

Ahlfors, R., Lång, S., Overmyer, K., Jaspers, P., Brosché, M., Tauriainen, A., ... & Inzé, D. (2004). Arabidopsis RADICAL-INDUCED CELL DEATH1 belongs to the WWE protein–protein interaction domain protein family and modulates abscisic acid, ethylene, and methyl jasmonate responses. *The Plant Cell*, *16*(7), 1925-1937.

Allen, J. F., & Forsberg, J. (2001). Molecular recognition in thylakoid structure and function. *Trends in plant science*, *6*(7), 317-326.

Amunts, A., Toporik, H., Borovikova, A., & Nelson, N. (2010). Structure determination and improved model of plant photosystem I. *Journal of Biological Chemistry*, *285*(5), 3478-3486.

Armbruster, U., Galvis, V. C., Kunz, H. H., & Strand, D. D. (2017). The regulation of the chloroplast proton motive force plays a key role for photosynthesis in fluctuating light. *Current opinion in plant biology*, *37*, 56-62.

Aro, E. M., Suorsa, M., Rokka, A., Allahverdiyeva, Y., Paakkarinen, V., Saleem, A., ... & Rintamäki, E. (2005). Dynamics of photosystem II: a proteomic approach to thylakoid protein complexes. *Journal of experimental botany*, *56*(411), 347-356.

Aro, E. M., Virgin, I., & Andersson, B. (1993). Photoinhibition of photosystem II. Inactivation, protein damage and turnover. *Biochimica et Biophysica Acta (BBA)-Bioenergetics*, *1143*(2), 113-134.

Asada, K. (2000). The water–water cycle as alternative photon and electron sinks. *Philosophical Transactions of the Royal Society of London. Series B: Biological Sciences*, *355*(1402), 1419-1431.

Asada, K., Urano, M., & Takahashi, M. A. (1973). Subcellular location of superoxide dismutase in spinach leaves and preparation and properties of crystalline spinach superoxide dismutase. *European Journal of Biochemistry*, *36*(1), 257-266.

Baker, N. R. (2008). Chlorophyll fluorescence: a probe of photosynthesis in vivo. *Annu. Rev. Plant Biol.*, *59*, 89-113.

Barber, J. (1989). Function and molecular biology of Photosystem two. *Oxford surveys of plant molecular and cell biology*.

Bilger, W., & Björkman, O. (1990). Role of the xanthophyll cycle in photoprotection elucidated by measurements of light-induced absorbance changes, fluorescence and photosynthesis in leaves of Hedera canar-

iensis. *Photosynthesis research*, *25*(3), 173-185.

Blanco, N. E., Guinea-Díaz, M., Whelan, J., & Strand, Å. (2014). Interaction between plastid and mitochondrial retrograde signalling pathways during changes to plastid redox status. *Philosophical Transactions of the Royal Society B: Biological Sciences*, *369*(1640), 20130231.

Boekema, E. J., Hankamer, B., Bald, D., Kruip, J., Nield, J., Boonstra, A. F., ... & Rögner, M. (1995). Supramolecular structure of the photosystem II complex from green plants and cyanobacteria. *Proceedings of the National Academy of Sciences*, *92*(1), 175-179.

Bradbeer, J. W., Atkinson, Y. E., Börner, T., & HAGEMANN, R. (1979). Cytoplasmic synthesis of plastid polypeptides may be controlled by plastid-synthesised RNA. *Nature*, *279*(5716), 816-817.

Breyton, C., Nandha, B., Johnson, G. N., Joliot, P., & Finazzi, G. (2006). Redox modulation of cyclic electron flow around photosystem I in C3 plants. *Biochemistry*, *45*(45), 13465-13475.

Bricker, T.M., Roose, J.L., Fagerlund, R.D., Frankel, L.K., and Eaton-Rye, J.J. (2012) The extrinsic proteins of Photosystem II. *Biochim Biophys Acta*. *1817*: 121–42.

Brody, S. S., & Brody, M. (1961). Absorption properties of aggregated (dimeric) chlorophyll. *Biochimica et biophysica acta*, *54*(3), 495-505.

Buchanan, B. B., Schürmann, P., Wolosiuk, R. A., & Jacquot, J. P. (2002). The ferredoxin/thioredoxin system: from discovery to molecular structures and beyond. *Photosynthesis Research*, *73*(1-3), 215-222.

Cao, P., Su, X., Pan, X., Liu, Z., Chang, W., & Li, M. (2018). Structure, assembly and energy transfer of plant photosystem II supercomplex. *Biochimica et Biophysica Acta (BBA)-Bioenergetics*, *1859*(9), 633-644.

Cardona, T., Murray, J. W., & Rutherford, A. W. (2015). Origin and evolution of water oxidation before the last common ancestor of the cyanobacteria. *Molecular biology and evolution*, *32*(5), 1310-1328.

Carrillo, L. R., Froehlich, J. E., Cruz, J. A., Savage, L. J., & Kramer, D. M. (2016). Multi-level regulation of the chloroplast ATP synthase: the chloroplast NADPH thioredoxin reductase C (NTRC) is required for redox modulation specifically under low irradiance. *The Plant Journal*, *87*(6), 654-663.

Chan, K. X., Mabbitt, P. D., Phua, S. Y., Mueller, J. W., Nisar, N., Gigolashvili, T., ... & Jackson, C. J. (2016). Sensing and signaling of oxidative stress in chloroplasts by inactivation of the SAL1 phosphoadenosine phosphatase. *Proceedings of the National Academy of Sciences*, *113*(31), E4567-E4576.

Courteille, A., Vesa, S., Sanz-Barrio, R., Cazalé, A. C., Becuwe-Linka, N., Farran, I., ... & Rumeau, D. (2013). Thioredoxin m4 controls photosynthetic

alternative electron pathways in Arabidopsis. *Plant Physiology*, *161*(1), 508-520.

Cramer, W. A., Zhang, H., Yan, J., Kurisu, G., & Smith, J. L. (2006). Transmembrane traffic in the cytochrome b 6 f complex. *Annu. Rev. Biochem.*, *75*, 769-790.

DalCorso, G., Pesaresi, P., Masiero, S., Aseeva, E., Schünemann, D., Finazzi, G., ... & Leister, D. (2008). A complex containing PGRL1 and PGR5 is involved in the switch between linear and cyclic electron flow in Arabidopsis. *Cell*, *132*(2), 273-285.

Danielsson, R., Suorsa, M., Paakkarinen, V., Albertsson, P. Å., Styring, S., Aro, E. M., & Mamedov, F. (2006). Dimeric and Monomeric Organization of Photosystem II distribution of five distinct complexes in the different domains of the thylakoid membrane. *Journal of Biological Chemistry*, *281*(20), 14241-14249.

De Clercq, I., Vermeirssen, V., Van Aken, O., Vandepoele, K., Murcha, M. W., Law, S. R., ... & Van De Cotte, B. (2013). The membrane-bound NAC transcription factor ANAC013 functions in mitochondrial retrograde regulation of the oxidative stress response in Arabidopsis. *The Plant Cell*, *25*(9), 3472-3490.

Dekker, J. P., & Boekema, E. J. (2005). Supramolecular organization of thylakoid membrane proteins in green plants. *Biochimica et Biophysica Acta (BBA)-Bioenergetics*, *1706*(1-2), 12-39.

Delwiche, C. F. (1999). Tracing the thread of plastid diversity through the tapestry of life. *the american naturalist*, *154*(S4), S164-S177.

Demmig-Adams, B. (1990). Carotenoids and photoprotection in plants: a role for the xanthophyll zeaxanthin. *Biochimica et Biophysica Acta (BBA)-Bioenergetics*, *1020*(1), 1-24.

Demmig, B., Winter, K., Krüger, A., & Czygan, F. C. (1987). Photoinhibition and zeaxanthin formation in intact leaves: a possible role of the xanthophyll cycle in the dissipation of excess light energy. *Plant physiology*, *84*(2), 218-224.

Depège, N., Bellafiore, S., & Rochaix, J. D. (2003). Role of chloroplast protein kinase Stt7 in LHCII phosphorylation and state transition in Chlamydomonas. *Science*, *299*(5612), 1572-1575.

Deusch, O., Landan, G., Roettger, M., Gruenheit, N., Kowallik, K. V., Allen, J. F., ... & Dagan, T. (2008). Genes of cyanobacterial origin in plant nuclear genomes point to a heterocyst-forming plastid ancestor. *Molecular biology and evolution*, *25*(4), 748-761.

Douglas, S. E. (1998). Plastid evolution: origins, diversity, trends. *Current opinion in genetics & development*, *8*(6), 655-661.

Douglas, A. E., & Raven, J. A. (2003). Genomes at the interface between bacteria and organelles. *Philosophical Transactions of the Royal Society of London. Series B: Biological Sciences*, *358*(1429), 5-18.

Droux, M., Jacquot, J. P., Miginac-Maslow, M., Gadal, P., Huet, J. C., Crawford, N. A., ... & Buchanan, B. B. (1987). Ferredoxin-thioredoxin reductase, an iron-sulfur enzyme linking light to enzyme regulation in oxygenic photosynthesis: purification and properties of the enzyme from C3, C4, and cyanobacterial species. *Archives of biochemistry and biophysics*, *252*(2), 426-439.

Edwards, G. E., & Walker, D. A. 1983C3, C4: mechanisms, and cellular and environmental regulation of photosynthesis.

Endo, T., Shikanai, T., Takabayashi, A., Asada, K., & Sato, F. (1999). The role of chloroplastic NAD (P) H dehydrogenase in photoprotection. *Febs Letters*, *457*(1), 5-8.

Estavillo, G. M., Crisp, P. A., Pornsiriwong, W., Wirtz, M., Collinge, D., Carrie, C., ... & Brearley, C. (2011). Evidence for a SAL1-PAP chloroplast retrograde pathway that functions in drought and high light signaling in Arabidopsis. *The Plant Cell*, *23*(11), 3992-4012.

Ettinger, W. F., & Theg, S. M. (1991). Physiologically active chloroplasts contain pools of unassembled extrinsic proteins of the photosynthetic oxygen-evolving enzyme complex in the thylakoid lumen. *The Journal of cell biology*, *115*(2), 321-328.

Fork, D. C., & Herbert, S. K. (1993). Electron transport and photophosphorylation by photosystem I in vivo in plants and cyanobacteria. *Photosynthesis research*, *36*(3), 149-168.

Fujibe, T., Saji, H., Arakawa, K., Yabe, N., Takeuchi, Y., & Yamamoto, K. T. (2004). A methyl viologen-resistant mutant of Arabidopsis, which is allelic to ozone-sensitive rcd1, is tolerant to supplemental ultraviolet-B irradiation. *Plant Physiology*, *134*(1), 275-285.

Govindjee, U. (2014). *Non-photochemical quenching and energy dissipation in plants, algae and cyanobacteria* (Vol. 40). B. Demmig-Adams, G. Garab, & W. Adams III (Eds.). Dordrecht, The Netherlands: Springer Netherlands.

Grieco, M., Suorsa, M., Jajoo, A., Tikkanen, M., & Aro, E. M. (2015). Light-harvesting II antenna trimers connect energetically the entire photosynthetic machinery—including both photosystems II and I. *Biochimica et Biophysica Acta (BBA)-Bioenergetics*, *1847*(6-7), 607-619.

Haehnel, W., Jansen, T., Gause, K., Klösgen, R. B., Stahl, B., Michl, D., ... & Herrmann, R. G. (1994). Electron transfer from plastocyanin to photosystem I. *The EMBO journal*, *13*(5), 1028-1038.

Hangarter, R. P., Grandoni, P., & Ort, D. R. (1987). The effects of chloroplast coupling factor reduction on the energetics of activation and on the energetics and efficiency of ATP formation. *Journal of Biological Chemistry*, *262*(28), 13513-13519.

Harrison, S. J., Mott, E. K., Parsley, K., Aspinall, S., Gray, J. C., & Cottage, A. (2006). A rapid and robust method of identifying transformed Arabidopsis

thaliana seedlings following floral dip transformation. *Plant methods*, *2*(1), 19.

Hashimoto, A., Ettinger, W. F., Yamamoto, Y., & Theg, S. M. (1997). Assembly of newly imported oxygen-evolving complex subunits in isolated chloroplasts: sites of assembly and mechanism of binding. *The Plant Cell*, *9*(3), 441-452.

Heber, U., & Walker, D. (1992). Concerning a dual function of coupled cyclic electron transport in leaves. *Plant Physiology*, *100*(4), 1621-1626.

Hohmann-Marriott, M. F., & Blankenship, R. E. (2011). Evolution of photosynthesis. *Annual review of plant biology*, *62*, 515-548.

Horton, P., Wentworth, M., & Ruban, A. (2005). Control of the light harvesting function of chloroplast membranes: The LHCII-aggregation model for non-photochemical quenching. *Febs Letters*, *579*(20), 4201-4206.

Ifuku, K., Endo, T., Shikanai, T., & Aro, E. M. (2011). Structure of the chloroplast NADH dehydrogenase-like complex: nomenclature for nuclear-encoded subunits. *Plant and cell physiology*, *52*(9), 1560-1568.

Ifuku, K., & Noguchi, T. (2016). Structural coupling of extrinsic proteins with the oxygen-evolving center in photosystem II. *Frontiers in plant science*, *7*, 84.

Isemer, R., Mulisch, M., Schäfer, A., Kirchner, S., Koop, H. U., & Krupinska, K. (2012). Recombinant Whirly1 translocates from transplastomic chloroplasts to the nucleus. *FEBS letters*, *586*(1), 85-88.

Ishihara, S., Takabayashi, A., Ido, K., Endo, T., Ifuku, K., & Sato, F. (2007). Distinct functions for the two PsbP-like proteins PPL1 and PPL2 in the chloroplast thylakoid lumen of Arabidopsis. *Plant physiology*, *145*(3), 668-679.

Ishikita, H., Loll, B., Biesiadka, J., Saenger, W., & Knapp, E. W. (2005). Redox potentials of chlorophylls in the photosystem II reaction center. *Biochemistry*, *44*(10), 4118-4124.

Iwai, M., Takizawa, K., Tokutsu, R., Okamuro, A., Takahashi, Y., & Minagawa, J. (2010). Isolation of the elusive supercomplex that drives cyclic electron flow in photosynthesis. *Nature*, *464*(7292), 1210-1213.

Jackowski, G., Kacprzak, K., & Jansson, S. (2001). Identification of Lhcb1/Lhcb2/Lhcb3 heterotrimers of the main light-harvesting chlorophyll a/b–protein complex of Photosystem II (LHC II). *Biochimica et Biophysica Acta (BBA)-Bioenergetics*, *1504*(2-3), 340-345.

Järvi, S., Gollan, P. J., & Aro, E. M. (2013). Understanding the roles of the thylakoid lumen in photosynthesis regulation. *Frontiers in plant science*, *4*, 434.

Järvi, S., Suorsa, M., Paakkarinen, V., & Aro, E. M. (2011). Optimized native gel systems for separation of thylakoid protein complexes: novel super-and mega-complexes. *Biochemical Journal*, *439*(2), 207-214.

Jaspers, P., Blomster, T., Brosché, M., Salojärvi, J., Ahlfors, R., Vainonen, J. P., ... & Overmyer, K. (2009). Unequally redundant RCD1 and SRO1 mediate stress and developmental responses and interact with transcription factors. *The Plant Journal*, *60*(2), 268-279.

Jaspers, P., Brosché, M., Overmyer, K., & Kangasjär, J. (2010). The transcription factor interacting protein RCD1 contains a novel conserved domain. *Plant signaling & behavior*, *5*(1), 78-80.

Jedmowski, C., & Brüggemann, W. (2015). Imaging of fast chlorophyll fluorescence induction curve (OJIP) parameters, applied in a screening study with wild barley (Hordeum spontaneum) genotypes under heat stress. *Journal of Photochemistry and Photobiology B: Biology*, *151*, 153-160.

Junesch, U., & Gräber, P. (1987). Influence of the redox state and the activation of the chloroplast ATP synthase on proton-transport-coupled ATP synthesis/hydrolysis. *Biochimica et Biophysica Acta (BBA)-Bioenergetics*, *893*(2), 275-288.

Kanazawa, A., & Kramer, D. M. (2002). In vivo modulation of nonphotochemical exciton quenching (NPQ) by regulation of the chloroplast ATP synthase. *Proceedings of the National Academy of Sciences*, *99*(20), 12789-12794.

Kangasjärvi, S., Neukermans, J., Li, S., Aro, E. M., & Noctor, G. (2012). Photosynthesis, photorespiration, and light signalling in defence responses. *Journal of experimental botany*, *63*(4), 1619-1636.

Kargul, J., & Barber, J. (2008). Photosynthetic acclimation: Structural reorganisation of light harvesting antenna–role of redox-dependent phosphorylation of major and minor chlorophyll a/b binding proteins. *The FEBS journal*, *275*(6), 1056-1068.

Kashino, Y., Lauber, W. M., Carroll, J. A., Wang, Q., Whitmarsh, J., Satoh, K., & Pakrasi, H. B. (2002). Proteomic analysis of a highly active photosystem II preparation from the cyanobacterium Synechocystis sp. PCC 6803 reveals the presence of novel polypeptides. *Biochemistry*, *41*(25), 8004-8012.

Kautsky, H., Appel, W., & Amann, H. (1960). Chlorophyll fluorescence and carbon assimilation. Part XIII. The fluorescence and the photochemistry of plants. *Biochemische Zeitschrift*, *332*, 277-292.

Keren, N., Ohkawa, H., Welsh, E. A., Liberton, M., & Pakrasi, H. B. (2005). Psb29, a conserved 22-kD protein, functions in the biogenesis of photosystem II complexes in Synechocystis and Arabidopsis. *The Plant Cell*, *17*(10), 2768-2781.

Ketcham, S. R., Davenport, J. W., Warncke, K., & McCarty, R. E. (1984). Role of the gamma subunit of chloroplast coupling factor 1 in the light-dependent activation of photophosphorylation and ATPase activity by dithiothreitol. *Journal of Biological Chemistry*, *259*(11), 7286-7293.

Kobayashi, M., Ohura, I., Kawakita, K., Yokota, N., Fujiwara, M., Shimamoto, K., ... & Yoshioka, H. (2007). Calcium-dependent protein kinases regu-

late the production of reactive oxygen species by potato NADPH oxidase. *The plant cell*, *19*(3), 1065-1080.

Kojima, K., Oshita, M., Nanjo, Y., Kasai, K., Tozawa, Y., Hayashi, H., & Nishiyama, Y. (2007). Oxidation of elongation factor G inhibits the synthesis of the D1 protein of photosystem II. *Molecular microbiology*, *65*(4), 936-947.

Kok, B., Forbush, B., & McGloin, M. (1970). Cooperation of charges in photosynthetic O2 evolution–I. A linear four step mechanism. *Photochemistry and Photobiology*, *11*(6), 457-475.

Konermann, L., & Holzwarth, A. R. (1996). Analysis of the absorption spectrum of photosystem II reaction centers: temperature dependence, pigment assignment, and inhomogeneous broadening. *Biochemistry*, *35*(3), 829-842.

Krieger-Liszkay, A. (2005). Singlet oxygen production in photosynthesis. *Journal of experimental botany*, *56*(411), 337-346.

Kroemer, G., Petit, P., Zamzami, N., Vayssière, J. L., & Mignotte, B. (1995). The biochemistry of programmed cell death. *The FASEB Journal*, *9*(13), 1277-1287.

Kühlbrandt, W., Wang, D. N., & Fujiyoshi, Y. (1994). Atomic model of plant light-harvesting complex by electron crystallography. *Nature*, *367*(6464), 614-621.

Kuhn, A., Stuart, R., Henry, R., & Dalbey, R. E. (2003). The Alb3/Oxa1/YidC protein family: membrane-localized chaperones facilitating membrane protein insertion?. *Trends in cell biology*, *13*(10), 510-516.

Küpper, H., Benedikty, Z., Morina, F., Andresen, E., Mishra, A., & Trtilek, M. (2019). Analysis of OJIP chlorophyll fluorescence kinetics and QA reoxidation kinetics by direct fast imaging. *Plant physiology*, *179*(2), 369-381.

Laemmli, U. K. (1970). Cleavage of structural proteins during the assembly of the head of bacteriophage T4. *nature*, *227*(5259), 680-685.

Lee, S. H., & Min, D. B. (1990). Effects, quenching mechanisms, and kinetics of carotenoids in chlorophyll-sensitized photooxidation of soybean oil. *Journal of Agricultural and Food Chemistry*, *38*(8), 1630-1634.

Lemeille, S., & Rochaix, J. D. (2010). State transitions at the crossroad of thylakoid signalling pathways. *Photosynthesis research*, *106*(1-2), 33-46.

Lemeille, S., Willig, A., Depege-Fargeix, N., Delessert, C., Bassi, R., & Rochaix, J. D. (2009). Analysis of the chloroplast protein kinase Stt7 during state transitions. *PLoS biology*, *7*(3).

Li, X. P., BjoÈrkman, O., Shih, C., Grossman, A. R., Rosenquist, M., Jansson, S., & Niyogi, K. K. (2000). A pigment-binding protein essential for regulation of photosynthetic light harvesting. *Nature*, *403*(6768), 391-395.

Liu, Z., Yan, H., Wang, K., Kuang, T., Zhang, J., Gui, L., ... & Chang, W. (2004). Crystal structure of spinach major light-harvesting complex at 2.72 Å

resolution. *Nature*, *428*(6980), 287-292.

Lowry, O. H., Rosebrough, N. J., Farr, A. L., & Randall, R. J. (1951). Protein measurement with the Folin phenol reagent. *Journal of biological chemistry*, *193*, 265-275.

Macpherson, A. N., Telfer, A., Barber, J., & Truscott, T. G. (1993). Direct detection of singlet oxygen from isolated photosystem II reaction centres. *Biochimica et Biophysica Acta (BBA)-Bioenergetics*, *1143*(3), 301-309.

Matsubayashi, T., Wakasugi, T., Shinozaki, K., Yamaguchi-Shinozaki, K., Zaita, N., Hidaka, T., ... & Maruyama, T. (1987). Six chloroplast genes (ndhA-F) homologous to human mitochondrial genes encoding components of the respiratory chain NADH dehydrogenase are actively expressed: determination of the splice sites in ndhA and ndhB pre-mRNAs. *Molecular and General Genetics MGG*, *210*(3), 385-393.

Matsuzaki, M., Misumi, O., Shin-i, T., Maruyama, S., Takahara, M., Miyagishima, S. Y., & Yoshida, Y. (2004). Genome sequence of the ultrasmall unicellular red alga Cyanidioschyzon merolae 10D. *Nature*, *428*(6983), 653-657.

McFadden, G. I., & van Dooren, G. G. (2004). Evolution: red algal genome affirms a common origin of all plastids. *Current biology*, *14*(13), R514-R516.

Mehler, A. H. (1951). Studies on reactions of illuminated chloroplasts: I. Mechanism of the reduction of oxygen and other hill reagents. *Archives of Biochemistry and Biophysics*, *33*(1), 65-77.

Mereschkowsky, C. (1905). Uber natur und ursprung der chromatophoren im pflanzenreiche. *Biologisches Centralblatt*, *25*, 293-604.

Michalska, J., Zauber, H., Buchanan, B. B., Cejudo, F. J., & Geigenberger, P. (2009). NTRC links built-in thioredoxin to light and sucrose in regulating starch synthesis in chloroplasts and amyloplasts. *Proceedings of the National Academy of Sciences*, *106*(24), 9908-9913.

Miller, G., Schlauch, K., Tam, R., Cortes, D., Torres, M. A., Shulaev, V., ... & Mittler, R. (2009). The plant NADPH oxidase RBOHD mediates rapid systemic signaling in response to diverse stimuli. *Science signaling*, *2*(84), ra45-ra45.

Miyao, M., & Murata, N. (1984). Role of the 33-kDa polypeptide in preserving Mn in the photosynthetic oxygen-evolution system and its replacement by chloride ions. *FEBS letters*, *170*(2), 350-354.

Miyao, M., & Murata, N. (1989). The mode of binding of three extrinsic proteins of 33 kDa, 23 kDa and 18 kDa in the photosystem II complex of spinach. *Biochimica et Biophysica Acta (BBA)-Bioenergetics*, *977*(3), 315-321.

Morel, J. B., & Dangl, J. L. (1997). The hypersensitive response and the induction of cell death in plants. *Cell Death & Differentiation*, *4*(8), 671-683.

Müh, F., Glöckner, C., Hellmich, J., & Zouni, A. (2012). Light-induced quinone reduction in photosystem II. *Biochimica Et Biophysica Acta (BBA)-Bioenergetics*, *1817*(1), 44-65.

Mulo, P., Sakurai, I., & Aro, E. M. (2012). Strategies for psbA gene expression in cyanobacteria, green algae and higher plants: from transcription to PSII repair. *Biochimica et Biophysica Acta (BBA)-Bioenergetics*, *1817*(1), 247-257.

Munekage, Y., Hashimoto, M., Miyake, C., Tomizawa, K. I., Endo, T., Tasaka, M., & Shikanai, T. (2004). Cyclic electron flow around photosystem I is essential for photosynthesis. *Nature*, *429*(6991), 579-582.

Munekage, Y., Hojo, M., Meurer, J., Endo, T., Tasaka, M., & Shikanai, T. (2002). PGR5 is involved in cyclic electron flow around photosystem I and is essential for photoprotection in Arabidopsis. *Cell*, *110*(3), 361-371.

Mustárdy, L., Buttle, K., Steinbach, G., & Garab, G. (2008). The three-dimensional network of the thylakoid membranes in plants: quasihelical model of the granum-stroma assembly. *The Plant Cell*, *20*(10), 2552-2557.

Nellaepalli, S., Kodru, S., Tirupathi, M., & Subramanyam, R. (2012). Anaerobiosis induced state transition: a non photochemical reduction of PQ pool mediated by NDH in Arabidopsis thaliana. *PloS one*, *7*(11).

Neuhaus, H. E., & Emes, M. J. (2000). Nonphotosynthetic metabolism in plastids. *Annual review of plant biology*, *51*(1), 111-140.

Nevo, R., Charuvi, D., Tsabari, O., & Reich, Z. (2012). Composition, architecture and dynamics of the photosynthetic apparatus in higher plants. *The Plant Journal*, *70*(1), 157-176.

Ng, S., Ivanova, A., Duncan, O., Law, S. R., Van Aken, O., De Clercq, I., ... & Walker, H. (2013). A membrane-bound NAC transcription factor, ANAC017, mediates mitochondrial retrograde signaling in Arabidopsis. *The Plant Cell*, *25*(9), 3450-3471.

Nikkanen, L., Toivola, J., Diaz, M. G., & Rintamäki, E. (2017). Chloroplast thioredoxin systems: prospects for improving photosynthesis. *Philosophical Transactions of the Royal Society B: Biological Sciences*, *372*(1730), 20160474.

Nikkanen, L., Toivola, J., & Rintamäki, E. (2016). Crosstalk between chloroplast thioredoxin systems in regulation of photosynthesis. *Plant, cell & environment*, *39*(8), 1691-1705.

Nikkanen, L., Toivola, J., Trotta, A., Diaz, M. G., Tikkanen, M., Aro, E. M., & Rintamäki, E. (2018). Regulation of cyclic electron flow by chloroplast NADPH-dependent thioredoxin system. *Plant direct*, *2*(11), e00093.

Nilkens, M., Kress, E., Lambrev, P., Miloslavina, Y., Müller, M., Holzwarth, A. R., & Jahns, P. (2010). Identification of a slowly inducible zeaxanthin-dependent component of non-photochemical quenching of chlorophyll fluorescence generated under steady-state conditions in Arabidop-

sis. *Biochimica et Biophysica Acta (BBA)-Bioenergetics*, *1797*(4), 466-475.

Nishiyama, Y., Allakhverdiev, S. I., & Murata, N. (2011). Protein synthesis is the primary target of reactive oxygen species in the photoinhibition of photosystem II. *Physiologia Plantarum*, *142*(1), 35-46.

Niyogi, K. K., Grossman, A. R., & Björkman, O. (1998). Arabidopsis mutants define a central role for the xanthophyll cycle in the regulation of photosynthetic energy conversion. *The plant cell*, *10*(7), 1121-1134.

Nowaczyk, M. M., Hebeler, R., Schlodder, E., Meyer, H. E., Warscheid, B., & Rögner, M. (2006). Psb27, a cyanobacterial lipoprotein, is involved in the repair cycle of photosystem II. *The Plant Cell*, *18*(11), 3121-3131.

Overmyer, K., Brosché, M., & Kangasjärvi, J. (2003). Reactive oxygen species and hormonal control of cell death. *Trends in plant science*, *8*(7), 335-342.

Overmyer, K., Tuominen, H., Kettunen, R., Betz, C., Langebartels, C., Sandermann, H., & Kangasjärvi, J. (2000). Ozone-sensitive Arabidopsis rcd1 mutant reveals opposite roles for ethylene and jasmonate signaling pathways in regulating superoxide-dependent cell death. *The Plant Cell*, *12*(10), 1849-1862.

Papageorgiou, G. (1968). Light-Induced Changes in the Fluorescence Yield of Chlorophyll a In Vivo: II. Chlorella pyrenoidosa. *Biophysical journal*, *8*(11), 1316-1328.

Papageorgiou, G. (1968). Light-induced changes in the fluorescence yield of chlorophyll a in vivo: I. Anacystis nidulans. *Biophysical journal*, *8*(11), 1299-1315.

Peltier, G., Aro, E. M., & Shikanai, T. (2016). NDH-1 and NDH-2 plastoquinone reductases in oxygenic photosynthesis. *Annual review of plant biology*, *67*, 55-80.

Peng, L., Fukao, Y., Fujiwara, M., Takami, T., & Shikanai, T. (2009). Efficient operation of NAD (P) H dehydrogenase requires supercomplex formation with photosystem I via minor LHCI in Arabidopsis. *The Plant Cell*, *21*(11), 3623-3640.

Peng, L., & Shikanai, T. (2011). Supercomplex formation with photosystem I is required for the stabilization of the chloroplast NADH dehydrogenase-like complex in Arabidopsis. *Plant physiology*, *155*(4), 1629-1639.

Peng, L., Shimizu, H., & Shikanai, T. (2008). The chloroplast NAD (P) H dehydrogenase complex interacts with photosystem I in Arabidopsis. *Journal of Biological Chemistry*, *283*(50), 34873-34879.

Pérez-Ruiz, J. M., Spínola, M. C., Kirchsteiger, K., Moreno, J., Sahrawy, M., & Cejudo, F. J. (2006). Rice NTRC is a high-efficiency redox system for chloroplast protection against oxidative damage. *The Plant Cell*, *18*(9), 2356-2368.

Porra, R. J., Thompson, W. A., & Kriedemann, P. E. (1989). Determination of accurate extinction coefficients and simultaneous equations for assaying chlorophylls a and b extracted with four different solvents: verification of the concentration of chlorophyll standards by atomic absorption spectroscopy. *Biochimica et Biophysica Acta (BBA)-Bioenergetics*, *975*(3), 384-394.

Puerto-Galán, L., Pérez-Ruiz, J. M., Guinea, M., & Cejudo, F. J. (2015). The contribution of NADPH thioredoxin reductase C (NTRC) and sulfiredoxin to 2-Cys peroxiredoxin overoxidation in Arabidopsis thaliana chloroplasts. *Journal of experimental botany*, *66*(10), 2957-2966.

Rabinowitch, E. I. (1945). *Photosynthesis and related processes. Vol. 1, Chemistry of photosynthesis, chemosynthesis and related processes in vitro and in vivo*. Interscience publ.

Rappaport, F., Guergova-Kuras, M., Nixon, P. J., Diner, B. A., & Lavergne, J. (2002). Kinetics and pathways of charge recombination in photosystem II. *Biochemistry*, *41*(26), 8518-8527.

Richter, A. S., Peter, E., Rothbart, M., Schlicke, H., Toivola, J., Rintamäki, E., & Grimm, B. (2013). Posttranslational influence of NADPH-dependent thioredoxin reductase C on enzymes in tetrapyrrole synthesis. *Plant physiology*, *162*(1), 63-73.

Rivero, L., Scholl, R., Holomuzki, N., Crist, D., Grotewold, E., & Brkljacic, J. (2014). Handling Arabidopsis plants: growth, preservation of seeds, transformation, and genetic crosses. In *Arabidopsis protocols* (pp. 3-25). Humana Press, Totowa, NJ.

Roose, J. L., Frankel, L. K., Mummadisetti, M. P., & Bricker, T. M. (2016). The extrinsic proteins of photosystem II: update. *Planta*, *243*(4), 889-908.

Roose, J. L., Kashino, Y., & Pakrasi, H. B. (2007). The PsbQ protein defines cyanobacterial Photosystem II complexes with highest activity and stability. *Proceedings of the National Academy of Sciences*, *104*(7), 2548-2553.

Ruban, A. V. (2012). *The photosynthetic membrane: molecular mechanisms and biophysics of light harvesting*. John Wiley & Sons.

Ruban, A. V., Johnson, M. P., & Duffy, C. D. (2012). The photoprotective molecular switch in the photosystem II antenna. *Biochimica et Biophysica Acta (BBA)-Bioenergetics*, *1817*(1), 167-181.

Sato, N. (2010). Phylogenomic and structural modeling analyses of the PsbP superfamily reveal multiple small segment additions in the evolution of photosystem II-associated PsbP protein in green plants. *Molecular phylogenetics and evolution*, *56*(1), 176-186.

Sato, S., Nakamura, Y., Kaneko, T., Asamizu, E., & Tabata, S. (1999). Complete structure of the chloroplast genome of Arabidopsis thaliana. *DNA research*, *6*(5), 283-290.

Schansker, G., Tóth, S. Z., & Strasser, R. J. (2006). Dark recovery of the Chl a

fluorescence transient (OJIP) after light adaptation: the qT-component of non-photochemical quenching is related to an activated photosystem I acceptor side. *Biochimica et Biophysica Acta (BBA)-Bioenergetics*, *1757*(7), 787-797.

Schöttler, M. A., Albus, C. A., & Bock, R. (2011). Photosystem I: its biogenesis and function in higher plants. *Journal of plant physiology*, *168*(12), 1452-1461.

Schreiber, U., Hormann, H., Neubauer, C., & Klughammer, C. (1995). Assessment of photosystem II photochemical quantum yield by chlorophyll fluorescence quenching analysis. *Functional Plant Biology*, *22*(2), 209-220.

Schroda, M., Vallon, O., Wollman, F. A., & Beck, C. F. (1999). A chloroplast-targeted heat shock protein 70 (HSP70) contributes to the photoprotection and repair of photosystem II during and after photoinhibition. *The Plant Cell*, *11*(6), 1165-1178.

Schubert, M., Petersson, U. A., Haas, B. J., Funk, C., Schröder, W. P., & Kieselbach, T. (2002). Proteome map of the chloroplast lumen of Arabidopsis thaliana. *Journal of Biological Chemistry*, *277*(10), 8354-8365.

Schürmann, P., & Buchanan, B. B. (2008). The ferredoxin/thioredoxin system of oxygenic photosynthesis. *Antioxidants & redox signaling*, *10*(7), 1235-1274.

Schürmann, P., & Jacquot, J. P. (2000). Plant thioredoxin systems revisited. *Annual review of plant biology*, *51*(1), 371-400.

Serrato, A. J., Pérez-Ruiz, J. M., Spínola, M. C., & Cejudo, F. J. (2004). A novel NADPH thioredoxin reductase, localized in the chloroplast, which deficiency causes hypersensitivity to abiotic stress in Arabidopsis thaliana. *Journal of Biological Chemistry*, *279*(42), 43821-43827.

Shapiguzov, A., Ingelsson, B., Samol, I., Andres, C., Kessler, F., Rochaix, J. D., ... & Goldschmidt-Clermont, M. (2010). The PPH1 phosphatase is specifically involved in LHCII dephosphorylation and state transitions in Arabidopsis. *Proceedings of the National Academy of Sciences*, *107*(10), 4782-4787.

Shapiguzov, A., Nikkanen, L., Fitzpatrick, D., Vainonen, J. P., Gossens, R., Alseekh, S., ... & Benedikty, Z. (2020). Dissecting the interaction of photosynthetic electron transfer with mitochondrial signalling and hypoxic response in the Arabidopsis rcd1 mutant. *Philosophical Transactions of the Royal Society B*, *375*(1801), 20190413.

Shapiguzov, A., Vainonen, J. P., Hunter, K., Tossavainen, H., Tiwari, A., Järvi, S., ... & Van Der Kelen, K. (2019). Arabidopsis RCD1 coordinates chloroplast and mitochondrial functions through interaction with ANAC transcription factors. *Elife*, *8*, e43284.

Shapiguzov, A., Vainonen, J., Wrzaczek, M., & Kangasjärvi, J. (2012). ROS-talk–how the apoplast, the chloroplast, and the nucleus get the message through. *Frontiers in plant science*, *3*, 292.

Shimoni, E., Rav-Hon, O., Ohad, I., Brumfeld, V., & Reich, Z. (2005). Three-dimensional organization of higher-plant chloroplast thylakoid membranes revealed by electron tomography. *The Plant Cell*, *17*(9), 2580-2586.

Sonoike, K. (1996). Degradation of psaB gene product, the reaction center subunit of photosystem I, is caused during photoinhibition of photosystem I: possible involvement of active oxygen species. *Plant Science*, *115*(2), 157-164.

Stirbet, A. (2011). On the relation between the Kautsky effect (chlorophyll a fluorescence induction) and photosystem II: basics and applications of the OJIP fluorescence transient. *Journal of Photochemistry and Photobiology B: Biology*, *104*(1-2), 236-257.

Strand, Å., Asami, T., Alonso, J., Ecker, J. R., & Chory, J. (2003). Chloroplast to nucleus communication triggered by accumulation of Mg-protoporphyrinIX. *Nature*, *421*(6918), 79-83.

Strasser, B. J., & Strasser, R. J. (1995). Measuring fast fluorescence transients to address environmental questions: the JIP test, P. Mathis (Ed.), Photosynthesis: From Light to Biosphere, Vol. V. In *Proceedings of the Xth International Photosynthesis Congress. Montpellier, France, Kluwer Academic Publishers, Dordrecht*.

Strasser, R.J., Tsimilli-Michael, M., Srivastava, A., Srivastava, A. (2005) Analysis of the chlorophyll *a* fluorescence transient. In: Papageorgiou GC, Govindjee (eds) Advances in photosynthesis and respiration. Chlorophyll *a*fluorescence: a signature of photosynthesis. Kluwer Acad. Publ, Dordrecht, pp 321–362

Sundberg, E., Slagter, J. G., Fridborg, I., Cleary, S. P., Robinson, C., & Coupland, G. (1997). ALBINO3, an Arabidopsis nuclear gene essential for chloroplast differentiation, encodes a chloroplast protein that shows homology to proteins present in bacterial membranes and yeast mitochondria. *The Plant Cell*, *9*(5), 717-730.

Suorsa, M., & Aro, E. M. (2007). Expression, assembly and auxiliary functions of photosystem II oxygen-evolving proteins in higher plants. *Photosynthesis Research*, *93*(1-3), 89-100.

Suorsa, M., Regel, R. E., Paakkarinen, V., Battchikova, N., Herrmann, R. G., & Aro, E. M. (2004). Protein assembly of photosystem II and accumulation of subcomplexes in the absence of low molecular mass subunits PsbL and PsbJ. *European Journal of Biochemistry*, *271*(1), 96-107.

Suorsa, M., Sirpiö, S., Allahverdiyeva, Y., Paakkarinen, V., Mamedov, F., Styring, S., & Aro, E. M. (2006). PsbR, a missing link in the assembly of the oxygen-evolving complex of plant photosystem II. *Journal of Biological Chemistry*, *281*(1), 145-150.

Tagawa, K., & Arnon, D. I. (1962). Ferredoxins as electron carriers in photosynthesis and in the biological production and consumption of hydrogen gas. *Nature*, *195*(4841), 537-543.

Tikkanen, M., Grieco, M., Kangasjärvi, S., & Aro, E. M. (2010). Thylakoid protein

phosphorylation in higher plant chloroplasts optimizes electron transfer under fluctuating light. *Plant Physiology*, *152*(2), 723-735.

Tiwari, A., Mamedov, F., Grieco, M., Suorsa, M., Jajoo, A., Styring, S., ... & Aro, E. M. (2016). Photodamage of iron–sulphur clusters in photosystem I induces non-photochemical energy dissipation. *Nature Plants*, *2*(4), 1-9.

Townsend, A. J., Saccon, F., Giovagnetti, V., Wilson, S., Ungerer, P., & Ruban, A. V. (2018). The causes of altered chlorophyll fluorescence quenching induction in the Arabidopsis mutant lacking all minor antenna complexes. *Biochimica et Biophysica Acta (BBA)-Bioenergetics*, *1859*(9), 666-675.

Trebst, A., Depka, B., & Holländer-Czytko, H. (2002). A specific role for tocopherol and of chemical singlet oxygen quenchers in the maintenance of photosystem II structure and function in Chlamydomonas reinhardtii. *FEBS letters*, *516*(1-3), 156-160.

Trebst, A., Depka, B., Jäger, J., & Oettmeier, W. (2004). Reversal of the inhibition of photosynthesis by herbicides affecting hydroxyphenylpyruvate dioxygenase by plastoquinone and tocopheryl derivatives in Chlamydomonas reinhardtii. *Pest Management Science: formerly Pesticide Science*, *60*(7), 669-674.

Tsimilli-Michael, M., & Strasser, R. J. (2013). The energy flux theory 35 years later: formulations and applications. *Photosynthesis research*, *117*(1-3), 289-320.

Van Aken, O., De Clercq, I., Ivanova, A., Law, S. R., Van Breusegem, F., Millar, A. H., & Whelan, J. (2016). Mitochondrial and chloroplast stress responses are modulated in distinct touch and chemical inhibition phases. *Plant physiology*, *171*(3), 2150-2165.

Van Aken, O., Ford, E., Lister, R., Huang, S., & Millar, A. H. (2016). Retrograde signalling caused by heritable mitochondrial dysfunction is partially mediated by ANAC017 and improves plant performance. *The Plant Journal*, *88*(4), 542-558.

Vener, A. V., Van Kan, P. J., Rich, P. R., Ohad, I., & Andersson, B. (1997). Plastoquinol at the quinol oxidation site of reduced cytochrome bf mediates signal transduction between light and protein phosphorylation: thylakoid protein kinase deactivation by a single-turnover flash. *Proceedings of the National Academy of Sciences*, *94*(4), 1585-1590.

Walker, D. (1987). *The use of the oxygen electrode and fluorescence probes in simple measurements of photosynthesis*(p. 212). Sheffield: Research Institute for Photosynthesis, University of Sheffield.

Wollman, F. A. (2001). State transitions reveal the dynamics and flexibility of the photosynthetic apparatus. *The EMBO journal*, *20*(14), 3623-3630.

Yamamoto, H., Peng, L., Fukao, Y., & Shikanai, T. (2011). An Src homology 3 domain-like fold protein forms a ferredoxin binding site for the chloroplast

NADH dehydrogenase-like complex in Arabidopsis. *The Plant Cell*, *23*(4), 1480-1493.

Yamamoto, H., & Shikanai, T. (2013). In planta mutagenesis of Src homology 3 domain-like fold of NdhS, a ferredoxin-binding subunit of the chloroplast NADH dehydrogenase-like complex in Arabidopsis A conserved arg-193 plays a critical role in ferredoxin binding. *Journal of Biological Chemistry*, *288*(51), 36328-36337.

Yamori, W., Makino, A., & Shikanai, T. (2016). A physiological role of cyclic electron transport around photosystem I in sustaining photosynthesis under fluctuating light in rice. *Scientific Reports*, *6*, 20147.

Yamori, W., Shikanai, T., & Makino, A. (2015). Photosystem I cyclic electron flow via chloroplast NADH dehydrogenase-like complex performs a physiological role for photosynthesis at low light. *Scientific reports*, *5*, 13908.

Yokthongwattana, K., Chrost, B., Behrman, S., Casper-Lindley, C., & Melis, A. (2001). Photosystem II damage and repair cycle in the green alga Dunaliella salina: involvement of a chloroplast-localized HSP70. *Plant and Cell Physiology*, *42*(12), 1389-1397.

Zhang, X., Henriques, R., Lin, S. S., Niu, Q. W., & Chua, N. H. (2006). Agrobacterium-mediated transformation of Arabidopsis thaliana using the floral dip method. *Nature protocols*, *1*(2), 641.

Zito, F., Finazzi, G., Delosme, R., Nitschke, W., Picot, D., & Wollman, F. A. (1999). The Qo site of cytochrome b6f complexes controls the activation of the LHCII kinase. *The EMBO journal*, *18*(11), 2961-2969.

Zulfugarov, I. S., Tovuu, A., Eu, Y. J., Dogsom, B., Poudyal, R. S., Nath, K., ... & An, G. (2014). Production of superoxide from Photosystem II in a rice (Oryza sativaL.) mutant lacking PsbS. *BMC plant biology*, *14*(1), 242.

10 Appendices

1 Primers used in the genotyping

For *ppd8* (SAIL_249_E03):
LP: GAAGACGTCAATGAGCCTGAG
RP: GGCCAGTTTGTTCTTAGTCCC
LP + RP (gene-specific) or LP + left border SAIL (T-DNA-specific).

For *rcd1-4* (GK-229D11):
LP: TAGTGTCTCATAGGATCGTTCTTG
RP: ggggtttttgctcctgtttc
LP + RP (gene-specific) or LP + left border GABI (T-DNA-specific).

rcd1 ntrc has been published previously by Shapiguzov et al. 2020.

Multiple Comparisons

Dependent Variable: VAR00002

Bonferroni

(I) VAR00001		Mean Difference (I-J)	Std. Error	Sig.	95% Confidence Interval	
					Lower Bound	Upper Bound
#28	Col-0	,796662655250*	.1049628350428	.000	.451750730809	1.141574579691
	ppd8	.106890757000	.1049628350428	1.000	-.238021167441	.451802681441
	rcd1	,835015098250*	.1049628350428	.000	.490103173809	1.179927022691
	rcd1 ppd8	.117568881000	.1049628350428	1.000	-.227343043441	.462480805441
Col-0	#28	-,796662655250*	.1049628350428	.000	-1.141574579691	-.451750730809
	ppd8	-,689771898250*	.1049628350428	.000	-1.034683822691	-.344859973809
	rcd1	.038352443000	.1049628350428	1.000	-.306559481441	.383264367441
	rcd1 ppd8	-,679093774250*	.1049628350428	.000	-1.024005698691	-.334181849809
ppd8	#28	-.106890757000	.1049628350428	1.000	-.451802681441	.238021167441
	Col-0	,689771898250*	.1049628350428	.000	.344859973809	1.034683822691
	rcd1	,728124341250*	.1049628350428	.000	.383212416809	1.073036265691
	rcd1 ppd8	.010678124000	.1049628350428	1.000	-.334233800441	.355590048441
rcd1	#28	-,835015098250*	.1049628350428	.000	-1.179927022691	-.490103173809
	Col-0	-.038352443000	.1049628350428	1.000	-.383264367441	.306559481441
	ppd8	-,728124341250*	.1049628350428	.000	-1.073036265691	-.383212416809
	rcd1 ppd8	-,717446217250*	.1049628350428	.000	-1.062358141691	-.372534292809
rcd1 ppd8	#28	-.117568881000	.1049628350428	1.000	-.462480805441	.227343043441
	Col-0	,679093774250*	.1049628350428	.000	.334181849809	1.024005698691
	ppd8	-.010678124000	.1049628350428	1.000	-.355590048441	.334233800441
	rcd1	,717446217250*	.1049628350428	.000	.372534292809	1.062358141691

Based on observed means.

The error term is Mean Square(Error) = ,022.

*. The mean difference is significant at the 0

3 Statistical analysis for figure 7B

Upper panel:

At 5 hour time point

(I) VAR00014		Mean Difference (I-J)	Std. Error	Sig.	95% Confidence Interval	
					Lower Bound	Upper Bound
Col-0	ppd8	,09825060733*	.020640160681	.001	.04265139495	.15384981972
	R2	.00241497517	.020640160681	1.000	-.05318423722	.05801418755
ppd8	Col-0	-,09825060733*	.020640160681	.001	-.15384981972	-.04265139495
	R2	-,09583563217*	.020640160681	.001	-.15143484455	-.04023641978
R2	Col-0	-.00241497517	.020640160681	1.000	-.05801418755	.05318423722
	ppd8	,09583563217*	.020640160681	.001	.04023641978	.15143484455

Based on observed means. The error term is Mean Square(Error) = ,001.

At 15 hour time point

Multiple Comparisons

Dependent Variable: VAR00015

Bonferroni

(I) VAR00014		Mean Difference (I-J)	Std. Error	Sig.	95% Confidence Interval	
					Lower Bound	Upper Bound
Col-0	ppd8	.14076172303	.077035228603	.263	-.06675110122	.34827454728
	R2	.07923296167	.077035228603	.960	-.12827986259	.28674578592
ppd8	Col-0	-.14076172303	.077035228603	.263	-.34827454728	.06675110122
	R2	-.06152876136	.077035228603	1.000	-.26904158562	.14598406289
R2	Col-0	-.07923296167	.077035228603	.960	-.28674578592	.12827986259
	ppd8	.06152876136	.077035228603	1.000	-.14598406289	.26904158562

Based on observed means. The error term is Mean Square(Error) = ,018.

Bottom panel:

At 5 hour time point

Multiple Comparisons

Dependent Variable: VAR00015

Bonferroni

(I) VAR00014		Mean Difference (I-J)	Std. Error	Sig.	95% Confidence Interval	
					Lower Bound	Upper Bound
dm	R #3	-,15935652718*	.026846919737	.000	-.23167513048	-.08703792388
	rcd1	-,14856210639*	.026846919737	.000	-.22088070968	-.07624350309
R #3	dm	,15935652718*	.026846919737	.000	.08703792388	.23167513048
	rcd1	.01079442079	.026846919737	1.000	-.06152418250	.08311302409
rcd1	dm	,14856210639*	.026846919737	.000	.07624350309	.22088070968
	R #3	-.01079442079	.026846919737	1.000	-.08311302409	.06152418250

Based on observed means. The error term is Mean Square(Error) = ,002.

*. The mean difference is significant at the 0

At 15 hour time point:

Multiple Comparisons

Dependent Variable: VAR00015

Bonferroni

(I) VAR00014		Mean Difference (I-J)	Std. Error	Sig.	95% Confidence Interval	
					Lower Bound	Upper Bound
dm	R #3	-,47683716138*	.099217393968	.001	-.74410295665	-.20957136610
	rcd1	-,48815881895*	.099217393968	.001	-.75542461423	-.22089302367
R #3	dm	,47683716138*	.099217393968	.001	.20957136610	.74410295665
	rcd1	-.01132165757	.099217393968	1.000	-.27858745285	.25594413770
rcd1	dm	,48815881895*	.099217393968	.001	.22089302367	.75542461423
	R #3	.01132165757	.099217393968	1.000	-.25594413770	.27858745285

Based on observed means. The error term is Mean Square(Error) = ,030.

*. The mean difference is significant at the 0

4 Statistical analysis for figure 8A

Multiple Comparisons

Dependent Variable: VAR00015

Bonferroni

(I) VAR00014		Mean Difference (I-J)	Std. Error	Sig.	95% Confidence Interval	
					Lower Bound	Upper Bound
Col-0	dm	-.11374514249	.092260041169	1.000	-.40461165014	.17712136516
	ppd8	-,34727872583*	.092260041169	.016	-.63814523348	-.05641221818
	rcd1	-.18267070711	.092260041169	.427	-.47353721475	.10819580054
dm	Col-0	.11374514249	.092260041169	1.000	-.17712136516	.40461165014
	ppd8	-.23353358334	.092260041169	.158	-.52440009099	.05733292431
	rcd1	-.06892556461	.092260041169	1.000	-.35979207226	.22194094303
ppd8	Col-0	,34727872583*	.092260041169	.016	.05641221818	.63814523348
	dm	.23353358334	.092260041169	.158	-.05733292431	.52440009099
	rcd1	.16460801873	.092260041169	.598	-.12625848892	.45547452637
rcd1	Col-0	.18267070711	.092260041169	.427	-.10819580054	.47353721475
	dm	.06892556461	.092260041169	1.000	-.22194094303	.35979207226
	ppd8	-.16460801873	.092260041169	.598	-.45547452637	.12625848892

Based on observed means. The error term is Mean Square(Error) = ,017.

*. The mean difference is significant at the 0

5 Statistical analysis for figure 8B

Multiple Comparisons

Dependent Variable: VAR00002

Bonferroni

(I) VAR00001		Mean Difference (I-J)	Std. Error	Sig.	95% Confidence Interval	
					Lower Bound	Upper Bound
DM	MV DM	,31851829688*	.029870177480	.000	.22434714655	.4126894472
	MV rcd1	,11955755964*	.029870177480	.011	.02538640931	.2137287099
	rcd1	-,26553064814*	.029870177480	.000	-.35970179847	-.1713594978
MV DM	DM	-,31851829688*	.029870177480	.000	-.41268944721	-.2243471465
	MV rcd1	-,19896073725*	.029870177480	.000	-.29313188758	-.1047895869
	rcd1	-,58404894502*	.029870177480	.000	-.67822009536	-.4898777946
MV rcd1	DM	-,11955755964*	.029870177480	.011	-.21372870997	-.0253864093
	MV DM	,19896073725*	.029870177480	.000	.10478958692	.2931318875
	rcd1	-,38508820778*	.029870177480	.000	-.47925935811	-.2909170574
rcd1	DM	,26553064814*	.029870177480	.000	.17135949781	.3597017984
	MV DM	,58404894502*	.029870177480	.000	.48987779469	.6782200953
	MV rcd1	,38508820778*	.029870177480	.000	.29091705745	.4792593581

Based on observed means. The error term is Mean Square(Error) = ,002.

*. The mean difference is significant at the 0

6 Statistical analysis for figure 10B

Multiple Comparisons

Dependent Variable: VAR00015

Bonferroni

(I) VAR00014		Mean Difference (I-J)	Std. Error	Sig.	95% Confidence Interval	
					Lower Bound	Upper Bound
Col-0	dm	-.11374514249	.413413903587	1.000	-1.47223917534	1.24474889036
	ppd8	-.34727872583	.413413903587	1.000	-1.70577275868	1.01121530702
	rcd1	-.18267070711	.413413903587	1.000	-1.54116473996	1.17582332574
	tm	-2,05668034918*	.413413903587	.002	-3.41517438203	-.69818631633
dm	Col-0	.11374514249	.413413903587	1.000	-1.24474889036	1.47223917534
	ppd8	-.23353358334	.413413903587	1.000	-1.59202761619	1.12496044951
	rcd1	-.06892556461	.413413903587	1.000	-1.42741959746	1.28956846824
	tm	-1,94293520669*	.413413903587	.003	-3.30142923954	-.58444117384
ppd8	Col-0	.34727872583	.413413903587	1.000	-1.01121530702	1.70577275868
	dm	.23353358334	.413413903587	1.000	-1.12496044951	1.59202761619
	rcd1	.16460801873	.413413903587	1.000	-1.19388601412	1.52310205158
	tm	-1,70940162335*	.413413903587	.009	-3.06789565620	-.35090759050
rcd1	Col-0	.18267070711	.413413903587	1.000	-1.17582332574	1.54116473996
	dm	.06892556461	.413413903587	1.000	-1.28956846824	1.42741959746
	ppd8	-.16460801873	.413413903587	1.000	-1.52310205158	1.19388601412
	tm	-1,87400964208*	.413413903587	.004	-3.23250367492	-.51551560923
tm	Col-0	2,05668034918*	.413413903587	.002	.69818631633	3.41517438203
	dm	1,94293520669*	.413413903587	.003	.58444117384	3.30142923954
	ppd8	1,70940162335*	.413413903587	.009	.35090759050	3.06789565620
	rcd1	1,87400964208*	.413413903587	.004	.51551560923	3.23250367492

Based on observed means. The error term is Mean Square(Error) = ,342.

*. The mean difference is significant at the 0

7 Statistical analysis for figure 10C

Multiple Comparisons

Dependent Variable: VAR00002

Bonferroni

(I) VAR00001		Mean Difference (I-J)	Std. Error	Sig.	95% Confidence Interval	
					Lower Bound	Upper Bound
mQ ntrc	mQ TM	1.488357173631	.6787387391848	.293	-.651489765198	3.6282041124
	MV ntrc	.233428565631	.6787387391848	1.000	-1.906418373198	2.3732755044
	MV TM	.860420465881	.6787387391848	1.000	-1.279426472948	3.0002674047
mQ TM	mQ ntrc	-1.488357173631	.6787387391848	.293	-3.628204112460	.6514897651
	MV ntrc	-1.254928608000	.6787387391848	.535	-3.394775546829	.8849183308
	MV TM	-.627936707750	.6787387391848	1.000	-2.767783646579	1.5119102310
MV ntrc	mQ ntrc	-.233428565631	.6787387391848	1.000	-2.373275504461	1.9064183731
	mQ TM	1.254928608000	.6787387391848	.535	-.884918330829	3.3947755468
	MV TM	.626991900250	.6787387391848	1.000	-1.512855038580	2.7668388390
MV TM	mQ ntrc	-.860420465881	.6787387391848	1.000	-3.000267404710	1.2794264729
	mQ TM	.627936707750	.6787387391848	1.000	-1.511910231079	2.7677836465
	MV ntrc	-.626991900250	.6787387391848	1.000	-2.766838839079	1.5128550385

Based on observed means. The error term is Mean Square(Error) = ,921.

8 Statistical analysis for figure 11A

Multiple Comparisons

Dependent Variable: VAR00002

Bonferroni

(I) VAR00001		Mean Difference (I-J)	Std. Error	Sig.	95% Confidence Interval	
					Lower Bound	Upper Bound
DM MV	rcd1	-,823440693639*	.0952831629793	.000	-1.123838140922	-.523043246
	rcd1 MV	-.089367943330	.0952831629793	1.000	-.389765390613	.211029503
	rcd1 pp	-,519378268290*	.0952831629793	.001	-.819775715573	-.218980821
rcd1	DM MV	,823440693639*	.0952831629793	.000	.523043246356	1.123838140
	rcd1 MV	,734072750308*	.0952831629793	.000	.433675303025	1.034470197
	rcd1 pp	,304062425348*	.0952831629793	.047	.003664978065	.604459872
rcd1 MV	DM MV	.089367943330	.0952831629793	1.000	-.211029503953	.389765390
	rcd1	-,734072750308*	.0952831629793	.000	-1.034470197591	-.433675303
	rcd1 pp	-,430010324960*	.0952831629793	.004	-.730407772243	-.129612877
rcd1 pp	DM MV	,519378268290*	.0952831629793	.001	.218980821007	.819775715
	rcd1	-,304062425348*	.0952831629793	.047	-.604459872631	-.003664978
	rcd1 MV	,430010324960*	.0952831629793	.004	.129612877677	.730407772

Based on observed means. The error term is Mean Square(Error) = ,018.